CLNS 95/1317
January, 1995

# Weak and Rare Decays

J. Ritchie Patterson

Newman Laboratory of Nuclear Studies, Cornell University, Ithaca NY 14853

**Abstract**

We review recent results on weak and rare decays.

## 1. Introduction

Experimental high energy physics focuses on understanding the strong interactions of quarks, probing the standard model and searching for new physics. This paper reports on some of the recent progress in the last two of these areas. First, we look at recent studies of weak decays that shed light on the standard model, concentrating on tests of lepton universality and determination of the elements of the Cabibbo-Kobayashi-Maskawa (CKM) quark mixing matrix. Second, we will look at various rare processes for signs of physics beyond the standard model. For further discussion of some of these issues, see the related papers by Forty [1] and Roudeau [2] in these proceedings.

## 2. The Weak Decays of Leptons

We will begin with the leptons. In particular, we ask whether the third generation, the tau and its neutrino, is a carbon copy of the first and second generations, albeit a rather heavy carbon copy. The experiments contributing to tau physics are listed in table 1. Their center of mass energies span from the tau production threshold at 3.6 GeV to 90 GeV. The higher energy experiments tend to have very pure tau event samples and excellent efficiency; those at lower energies are able to distinguish the individual particles in a final state easily. As we shall see, BES, running at the tau pair production threshold, is uniquely able to determine the tau mass with high precision. In recent years there has been impressive progress in tau physics, and the complementarity among the experiments is partially responsible.

| Collab. | Accelerator | $E_{CM}$ (GeV) | $e^+e^- \to \tau^+\tau^-$ events |
|---|---|---|---|
| BES | BEPC | 3.6 | 500 |
| | | 4.0 | 54,000 |
| ARGUS | DORIS | 10.6 | 450,000 |
| CLEO | CESR | 10.6 | 2,500,000 |
| TPC/2$\gamma$ | PEP | 29 | 16,000 |
| ALEPH | LEP | 90 | 50,000 |
| DELPHI | LEP | 90 | 50,000 |
| L3 | LEP | 90 | 50,000 |
| OPAL | LEP | 90 | 50,000 |
| SLD | SLC | 90 | 1,600 |

**Table 1.** Current experiments in tau physics.

We first ask whether the strength of the coupling

*To appear in the Proceedings of the XXVII International Conference on High Energy Physics, Glasgow, Scotland, July, 1994.*

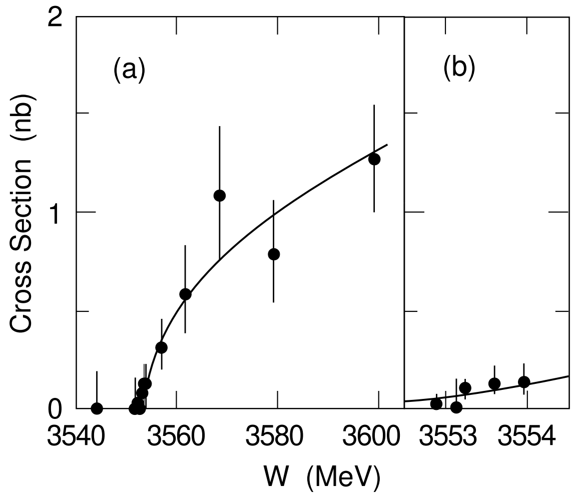


**Figure 1.** The tau-pair production cross section as a function of center of mass energy for the data (filled circles) and the fit (curve). The plot on the right is an expanded view of the threshold region (BES).

| Collab. | Year | | Result (MeV/$c^2$) |
|---|---|---|---|
| DASP | 1978 | [5] | $1807 \pm 20$ |
| SPEC | 1978 | [6] | $1787^{+10}_{-18}$ |
| DELCO | 1978 | [7] | $1783^{+3}_{-4}$ |
| MARK II | 1980 | [8] | $1787 \pm 10$ |
| BES† | 1992 | [4] | $1776.9^{+0.4}_{-0.5} \pm 0.2$ |
| ARGUS | 1992 | [9] | $1776.3 \pm 2.4 \pm 1.4$ |
| CLEO | 1992 | [10] | $1777.8 \pm 0.7 \pm 1.7$ |
| BES | 1994 | [3] | $1776.96^{+0.18+0.20}_{-0.19-0.16}$ |
| World Average | | | $1777.00 \pm 0.26$MeV/$c^2$ |

†This result is superseded by BES 1994.

**Table 2.** Experimental values of the tau mass.

| Expt. | Year | | Result (fs) |
|---|---|---|---|
| CLEO | 1987 | [14] | $325 \pm 14 \pm 18$ |
| MAC | 1987 | [15] | $309 \pm 17 \pm 7$ |
| ARGUS | 1987 | [16] | $295 \pm 14 \pm 11$ |
| HRS | 1987 | [17] | $299 \pm 14 \pm 11$ |
| TASSO | 1988 | [18] | $306 \pm 20 \pm 14$ |
| MARK II | 1988 | [19] | $288 \pm 16 \pm 17$ |
| JADE | 1989 | [20] | $301 \pm 29$ |
| CLEO | 1992 | [21] | $304 \pm 14 \pm 7$ |
| DELPHI | 1994 | [13] | $298 \pm 5$ |
| CLEO | 1994 | [22] | $291 \pm 4 \pm 7$ |
| CLEO | 1994 | [22] | $285 \pm 13 \pm 10$ |
| SLD | 1994 | [23] | $289 \pm 13 \pm 6$ |
| SLD | 1994 | [24] | $272 \pm 17 \pm 3$ |
| ALEPH | 1994 | [12] | $292.5 \pm 2.8 \pm 1.5$ |
| OPAL | 1994 | [11] | $288.8 \pm 2.2 \pm 1.4$ |
| World Average | | | $291.6 \pm 1.7$ fs |

**Table 3.** Experimental values of the tau lifetime.

of the $\tau$ to the $W$ is the same as that of the $e$ and $\mu$ to the $W$. We use the ratio of rates

$$\frac{\Gamma(\tau \to e\nu\bar{\nu})}{\Gamma(\mu \to e\nu\bar{\nu})} = \frac{\tau_\mu}{\tau_\tau} B_e = \frac{g_\tau^2}{g_\mu^2} \left( \frac{m_\tau}{m_\mu} \right)^5 ,$$

where $B_e$ is the tau electronic branching fraction and $m_\tau (m_\mu)$ and $\tau_\tau(\tau_\mu)$ are the $\tau(\mu)$ mass and lifetime. Since the parameters relating to the $\mu$ are well-known, our knowledge of $B_e$, $m_\tau$ and $\tau_\tau$ determines the precision of the test. At this conference new results were presented on all of these parameters.

The first result, and perhaps the most stunning, is a much more precise determination of the $\tau$ mass by BES [3], based on further analysis of their scan of the tau pair production threshold at the BEPC collider[4]. They measure the $e^+e^- \to \tau^+\tau^-$ production cross section as a function of energy, detecting the $\tau$'s through their decays to $e\nu\bar{\nu}$, $\mu\nu\bar{\nu}$, $\pi\nu$ or $K\nu$ (the old analysis used only $e\nu\bar{\nu}$ vs $\mu\nu\bar{\nu}$), and find the distribution shown in figure 1. They fit the predicted cross section versus energy to their data to extract the $\tau$ mass. The resulting curve agrees well with their data, and gives the result $m_\tau = 1776.96^{+0.18+0.20}_{-0.19-0.16}$ MeV/$c^2$. Measurements of $m_\tau$ are summarized in table 2. The world average is $1777.00 \pm 0.26$ MeV/$c^2$, and it is dominated by this measurement.

The tau lifetime results are summarized in table 3. The most precise values come from OPAL [11], ALEPH [12] and DELPHI [13], thanks to their silicon vertex detectors. OPAL selects $\tau$ decays to three charged particles, reconstructs the position of the decay vertex and calculates its separation from the interaction point. This distribution is shown in figure 2 for their 1992 and 1993 data samples. From it, they find $\tau_\tau = 288.9 \pm 3.6 \pm 1.7$ fs. They also extract the tau lifetime from the distance of closest approach of charged particles to the interaction point (i.e., the impact parameter) for one-prong $\tau$ decays. Combining these two results with those from their previous data samples yields the result $288.8 \pm 2.2 \pm 1.4$ fs. The OPAL value has been averaged with those of the other experiments with correlations in their systematic errors taken into account according to the procedure of Wasserbaech [25] and updated by Timmermans [26] at this conference. The world average value is $291.6 \pm 1.7$ fs.

The final ingredient in the analysis of the coupling constants is $B_e$, for which the LEP experiments DELPHI and ALEPH reported new measurements [27] [28]. The lepton spectrum from the ALEPH analysis is shown in figure 3. ALEPH finds a lower result than they have in the past, which they attribute to improved subtraction of hadrons

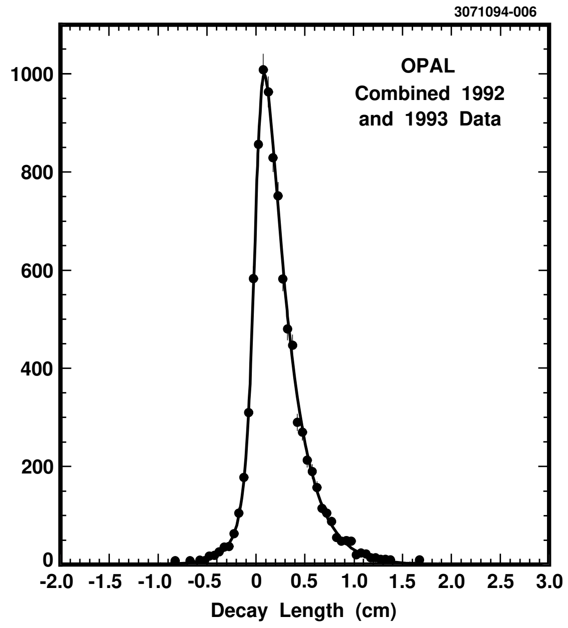


**Figure 2.** The $\tau$ decay length distribution for 3-prong decays (OPAL).

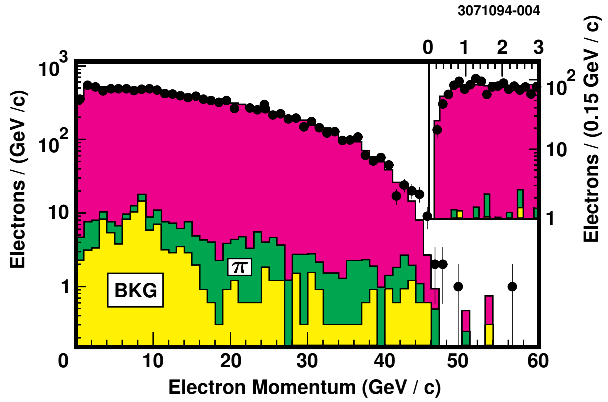


**Figure 3.** The momentum spectrum of electrons from $\tau \rightarrow e\nu\bar{\nu}$ for the data (filled circles), the Monte Carlo simulation (dark histogram), with backgrounds indicated from $\pi$ mis-identification (medium gray shading) and non-$\tau$ sources (light gray shading) (ALEPH).

misidentified as electrons and improved Monte Carlo simulation of the bhabha background after the inclusion of higher order radiative corrections. Remarkably, even though the precision is better than 1%, they are limited by their statistical rather than systematic uncertainty. The results of ALEPH and of the other collaborations are shown in table 2.

Combining the values for $m_\tau$, $\tau_\tau$ and $B_e$ we find the ratio of coupling constants $g_\tau/g_\mu = 0.994 \pm 0.004$. This result represents a noticeable shift since the ICHEP conference of two years ago, when the world average value was $g_\tau/g_\mu = 0.987 \pm 0.006$ [45]; the new result is compatible with $\tau$-$\mu$ universality.

| Expt. | Year | | Result (%) |
|---|---|---|---|
| DELCO | 1978 | [7] | $16.0 \pm 13$ |
| CELLO | 1983 | [29] | $18.3 \pm 2.4 \pm 1.9$ |
| PLUTO | 1985 | [30] | $13.0 \pm 1.9 \pm 2.9$ |
| MARK III | 1985 | [31] | $18.2 \pm 0.7 \pm 0.5$ |
| MAC | 1985 | [32] | $17.8 \pm 0.7 \pm 0.5$ |
| TASSO | 1985 | [33] | $20.4 \pm 3.0^{+1.4}_{-0.9}$ |
| JADE | 1986 | [34] | $16.8 \pm 0.7 \pm 0.9$ |
| MARK II | 1987 | [35] | $19.1 \pm 0.8 \pm 1.1$ |
| TPC | 1987 | [36] | $18.4 \pm 1.2 \pm 1.0$ |
| CRYSTAL BALL | 1989 | [37] | $16.3 \pm 0.3 \pm 3.2$ |
| CELLO | 1990 | [38] | $18.4 \pm 0.8 \pm 0.4$ |
| HRS | 1990 | [39] | $17.0 \pm 0.5 \pm 0.6$ |
| CLEO | 1992 | [40] | $19.1 \pm 0.4 \pm 0.6$ |
| CLEO | 1992 | [41] | $17.97 \pm 0.14 \pm 0.23$ |
| OPAL | 1992 | [42] | $17.50 \pm 0.3 \pm 0.3$ |
| ARGUS | 1993 | [43] | $17.5 \pm 0.3 \pm 0.5$ |
| L3 | 1993 | [44] | $17.86 \pm 0.25 \pm 0.23$ |
| DELPHI | 1994 | [27] | $17.61 \pm 0.22 \pm 0.40$ |
| ALEPH | 1994 | [28] | $17.48 \pm 0.15 \pm 0.06$ |
| | World Average | | $17.66 \pm 0.11$ % |

**Table 4.** Experimental values of the branching fraction of $\tau \rightarrow e\nu\bar{\nu}$.

Previous experiments have also measured the ratios of couplings $g_\mu/g_e = 1.0030 \pm 0.0023$ [46] and $g_e/g_\tau = 1.01 \pm 0.05$ [47]. We can summarize all of these results using the "universality triangle" shown in figure 4. The ratio $g_\tau/g_\mu$ is plotted on a logarithmic scale on the horizontal axis, with the vertical bars representing the $\pm 1$ standard deviation range. The values of $g_\mu/g_e$ and $g_e/g_\tau$ are similarly plotted along the other two sides of the triangle. If lepton universality holds, then the three bands should intersect at the center of the triangle. On the other hand, if the coupling strength of one lepton deviates from those of the other two, the overlap region will move toward one of the corners of the triangle. Currently the overlap region does not include the center of the triangle, but the difference is not significant.

We now turn from the magnitude of the coupling constant $g_\tau$ to the question of whether the coupling is $V - A$ in nature. If one allows all couplings (right-handed or left-handed combined with scalar, pseudoscalar, vector, axial vector or tensor), the leptonic decay rate of the tau is given by the expression [48]

$$\frac{\Gamma(\tau \rightarrow \ell\nu\bar{\nu})}{d\Omega dx} \propto x^2 g_\ell^2 g_\tau^2 \Big[ \quad 12(1-x) + \rho\left(\frac{32x}{3} - 8\right) + \eta \frac{m_\ell}{m_\tau}\frac{24(1-x)}{x} - P_\tau \xi \cos\theta \left(4(1-x) + \delta\left(\frac{32x}{3} - 8\right)\right)\Big],$$

where the parameters $\rho, \mu, \xi$ and $\delta$, called the

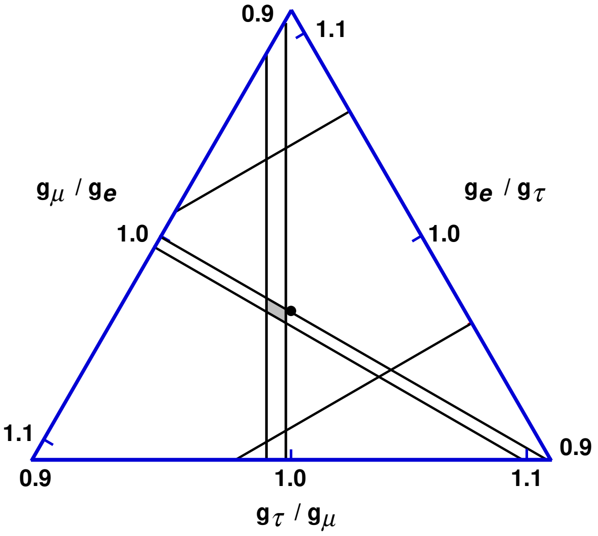


**Figure 4.** The "Universality triangle." If the couplings of the $e^\pm$, $\mu^\pm$ and $\tau^\pm$ to the $W$ boson have equal strength then bands indicating the measured ratios of the coupling constants should intersect at the center of the triangle (filled circle).

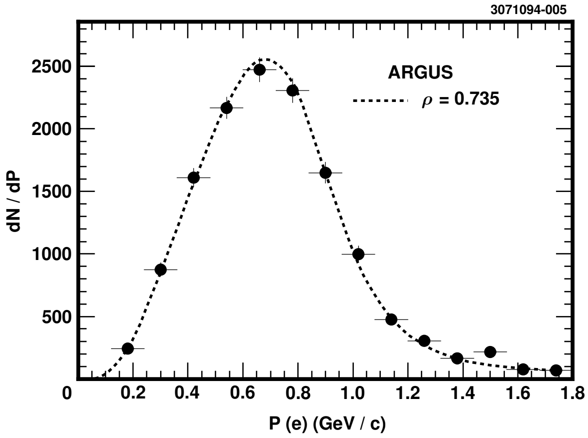


**Figure 5.** The electron momentum spectrum used to extract the Michel parameter $\rho$. The filled circles are the data and the curve is the result of the fit (ARGUS).

Michel parameters, are combinations of the ten coupling constants, $x$ is the normalized momentum of the daughter lepton, $x = p_\ell/E_\tau$, and $P_\tau$ is the tau polarization. The values of $\rho$ and $\eta$ can be determined from the $x$ distribution in leptonic decays, while determination of $\xi$ and $\delta$ requires knowledge of $P_\tau$.

ARGUS has extracted the values of $\rho$ and $\eta$ [49]. They use the fact that the muon spectrum is sensitive to the values of both $\rho$ and $\eta$, while the electron spectrum is sensitive only to $\rho$ because the coefficient $m_e/m_\tau$ suppresses the $\eta$ term. To increase their sensitivity, they boost the lepton into the rest frame of the $\tau$, having estimated the boost of the $\tau$ from the beam energy and the flight direction of the decay products of the opposite $\tau$. The resulting momentum spectrum for electrons is shown in figure 5 with the fit superimposed. They find $\rho = 0.735 \pm 0.036 \pm 0.020$ and $\eta = 0.03 \pm 0.18 \pm 0.12$. This value of $\rho$ is the most precise to date (though there is stiff competition from a recent ALEPH analysis) and this value of $\eta$ is the first obtained using this technique†. L3 has taken advantage of the polarization of LEP to extract the Michel parameters $\xi$ and $\delta$ [51]. The Michel parameter measurements are summarized in table 5.

The helicity of $\nu_\tau$ can be extracted from the kinematics of tau decays using the hadronic channels. To see how this is done, consider the decay $\tau \to \pi\nu$. Suppose a $\tau^-$ is traveling to the right, with its spin pointing in the direction of motion as shown in figure 6. If it decays to $\pi^-\nu_\tau$, then to conserve angular momentum the spin of the neutrino must also point to the right. If the neutrino is left-handed, the neutrino will emerge backward in the tau rest frame, and the $\pi$ will move forward. In the lab frame, the $\pi$ will be boosted, and have large momentum. On the other hand, if the neutrino were right-handed the $\pi$ spectrum would be soft in the lab frame. While the tau polarization is unknown event by event, the spins of $\tau$'s produced in $e^+e^-$ annihilation into a (spin 1) $Z^0$ or $\gamma^*$ are aligned, and consequently correlations between the energies of the pions from the decays of a $\tau^+\tau^-$ pair can reveal the helicity of the $\tau$ neutrino (though pure left-handed cannot be distinguished from pure right-handed.) CLEO has done such an analysis [59], while ARGUS has used both the angular and energy correlations of the products of $\tau \to \rho\nu$ decay [60], and ALEPH has done a fit to the energies of the decay products from $e\nu\bar{\nu}$, $\mu\nu\bar{\nu}$, $\pi\nu$ and $\rho\nu$ channels to extract simultaneously all the Michel parameters and the $\nu_\tau$ helicity [55]. The results on the helicity of $\nu_\tau$ are also summarized in table 5. Within the errors, both $\tau$'s and $\mu$'s support the standard model predictions.

Finally, we briefly review the status of the $\tau$ branching fractions. Recent results are given in table 6, table 7 and table 8. Many experiments do not distinguish between $\pi^-$'s and $K^-$'s, so they have been combined as $h^-$. Two caveats are required in interpreting the branching fractions. First, there is some ambiguity in categorizing final states that include a $K_L$ or $K_S$. For example, some analyses treat a $K_S \to \pi^+\pi^-$ decay as one neutral hadron while others treat it as two charged hadrons.

† The value of $\eta$ can also be inferred from the muonic decay rate. This gives a value of $0.01 \pm 0.05$ [50].

| Parameter | Result | Expt. | | | Tau average | Muon average | $V-A$ Pred. |
|---|---|---|---|---|---|---|---|
| $\rho$ | $0.71 \pm 0.09 \pm 0.03$ | CLEO | 1985 | [52] | | | |
| | $0.79 \pm 0.10 \pm 0.10$ | MAC | 1987 | [53] | | | |
| | $0.742 \pm 0.035 \pm 0.020$ | ARGUS | 1990 | [54] | | | |
| | $0.798 \pm 0.032 \pm 0.026$ | ALEPH | 1994 | [55] | | | |
| | $0.735 \pm 0.036 \pm 0.020$ | ARGUS | 1994 | [49] | | | |
| | | | | | $0.757 \pm 0.024$ | $0.7518 \pm 0.0026$ [56] | 0.75 |
| $\eta$ | $0.03 \pm 0.18 \pm 0.12$ | ARGUS | 1994 | [49] | $0.03 \pm 0.18 \pm 0.12$ | $-0.007 \pm 0.013$ [56] | 0 |
| $\xi$ | $0.90 \pm 0.15 \pm 0.10$ | ARGUS | 1993 | [57] | | | |
| | $1.13 \pm 0.17 \pm 0.07$ | ALEPH | 1994 | [55] | | | |
| | $1.29 \pm 0.49$ | L3 | 1994 | [51] | | | |
| | | | | | $1.03 \pm 0.12$ | $1.003 \pm 0.008$ [56] | 1 |
| $\delta$ | $0.79 \pm 0.17 \pm 0.06$ | ALEPH | 1994 | [55] | | | |
| | $0.38 \pm 0.57$ | L3 | 1994 | [51] | | | |
| | | | | | $0.75 \pm 0.17$ | $0.7486 \pm 0.0026 \pm 0.0028$ [56] | 0.75 |
| $\lvert\nu_\tau\text{helicity}\rvert$ | $1.25 \pm 0.23^{+0.23}_{-0.08}$ | ARGUS | 1993 | [58] | | | |
| | $0.99 \pm 0.06 \pm 0.09$ | CLEO | 1994 | [59] | | | |
| | $1.022 \pm 0.028 \pm 0.030$ | ARGUS | 1994 | [60] | | | |
| | $0.951 \pm 0.051 \pm 0.028$ | ALEPH | 1994 | [55] | | | |
| | | | | | $1.002 \pm 0.032$ | | 1 |

**Table 5.** Summary of the Michel Parameters and the $|\nu_\tau \text{helicity}|$ for $\tau$ and $\mu$ decay.

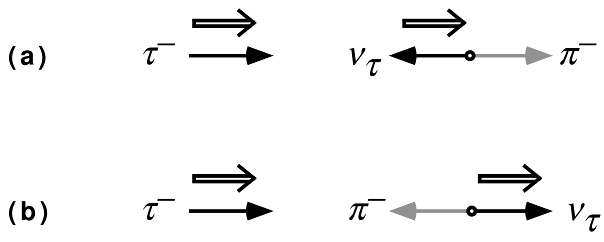


**Figure 6.** The decay $\tau \to \pi^- \nu_\tau$, with the spin (double arrow) of the $\tau$ and $\nu_\tau$ shown for (a) a left-handed $\nu_\tau$ and (b) a right-handed $\nu_\tau$.

Consequently, branching fractions reported by two experiments that purport to measure the same mode may actually refer to different final states. In table 9, modes with $K^0$'s are listed separately and the $K^0$ contribution has been subtracted from other results if their treatment of $K^0$'s was explicit. Second, many of the world averages are based on numerous measurements, and there has been no attempt to take into account the correlations in their systematic errors.

Because all of the major branching fractions have been measured, one can check that they sum to unity. A statistically significant shortfall could indicate a mismeasurement of one or more modes, an underestimate of the total error (perhaps as a consequence of neglecting correlations between different results when calculating the world averages), or, possibly, could point to one or more unexpected decay modes. The new world averages for principle decay modes are summarized in table 9. Most of the large branching fractions are known with a precision of order 1%. The total is $(98.2 \pm 0.7)\%$, a $(1.7 \pm 0.7)\%$ shortfall. To isolate the discrepancy, one can take a look at the "topological" branching fractions, that is, the inclusive branching fraction of $\tau$s to all final states with exactly one, three or five charged particles. For the one-prong decays we compare the sum of exclusive branching fractions, $(84.5 \pm 0.6)\%$, with the one- prong branching fraction, $(85.3 \pm 0.2)\%$. The two agree within approximately one standard deviation. This is a change from several years ago, in part because of a huge effort to improve the one-prong measurements. The three-prong modes are only recently gaining this attention, and here we currently see a significant discrepancy. It will be interesting to see what the next few years bring on this front.

## 3. The Weak Decays of Quarks

We move now to the quark sector, with an emphasis on new measurements of the CKM matrix elements. Measurement of the CKM matrix elements is important for four reasons. The first is technical convenience: to predict the decay rates of processes we have not observed, and to extract other information from the rates we measure. The second is to test the unitarity of the CKM matrix, the third is to explore $CP$ violation, which in the standard model arises from the complex part of the CKM matrix, and the final purpose is to constrain new theories that hope to predict the parameters of the standard model. At this conference there are

| Mode | Branching fraction (%) | Expt. | Data sample | | Comments |
|---|---|---|---|---|---|
| $e\nu\bar{\nu}$ | See table 2 | | | | |
| $\mu\nu\bar{\nu}$ | $17.05 \pm 0.14 \pm 0.06$ | ALEPH | 1991,92 | [28] | |
| | $16.80 \pm 0.32 \pm 0.26$ | OPAL | 1990,91 | [42] | |
| | $17.26 \pm 0.25 \pm 0.23$ | L3 | | [44] | |
| | $17.47 \pm 0.19 \pm 0.27$ | DELPHI | 1990-92 | [27] | |
| $h^-\nu$ | $12.04 \pm 0.34$ | ALEPH | 1989-91 | [61] | Excludes $K^* \to K_L\pi^-$ |
| | $12.20 \pm 0.3 \pm 0.4$ | OPAL | | [62] | Excludes $K^* \to K_L\pi^-$ |
| | $12.18 \pm 0.26 \pm 0.42$ | L3 | 1992 | [63] | |
| | $11.85 \pm 0.26 \pm 0.49$ | DELPHI | | [27] | Excludes $K^* \to K_L\pi^-$ |
| $h^-\pi^0\nu$ | $23.82 \pm 0.32 \pm 0.61$ | DELPHI | 1990,91,92 | [27] | Excludes $K^* \to K^-\pi^0$ |
| | $26.25 \pm 0.36 \pm 0.52$ | OPAL | 1991,92 | [64] | Includes $K^* \to K^-\pi^0$; Included in PDG94. |
| | $25.50 \pm 0.55$ | ALEPH | 1989-91 | [61] | Includes $K^* \to K^-\pi^0$ |
| | $25.87 \pm 0.12 \pm 0.42$ | CLEO | | [65] | Includes $K^* \to K^-\pi^0$; Included in PDG94. |
| | $25.20 \pm 0.35 \pm 0.50$ | L3 | 1992 | [63] | |
| $h^- \geq 2\pi^0\nu$ | $9.89 \pm 0.34 \pm 0.55$ | OPAL | 1991,92 | [64] | Includes $K_S \to 2\pi^0$ |
| $h^-2\pi^0\nu$ | $10.28 \pm 0.56$ | ALEPH | 1990,91 | [61] | Includes $K_S \to 2\pi^0$ |
| | $8.88 \pm 0.37 \pm 0.42$ | L3 | 1992 | [63] | |
| | $9.7 \pm 0.5 \pm 0.3$ | ARGUS | | [66] | |
| $h^-3\pi^0\nu$ | $1.70 \pm 0.24 \pm 0.40$ | L3 | 1992 | [63] | |
| | $1.7 \pm 0.3 \pm 0.2$ | ARGUS | | [66] | |
| $h^-h^+h^-\nu$ | $9.82 \pm 0.09 \pm 0.34$ | CLEO | | [67] | Excludes $K_S \to \pi^+\pi^-$ |
| | $9.56 \pm 0.24 \pm 0.22$ | ALEPH | 1991 | [61] | Excludes $K_S \to \pi^+\pi^-$ |
| $\pi^-\pi^+\pi^-\nu$ | $8.35 \pm 0.35 \pm 0.24$ | DELPHI | 1991 | [27] | They also find $M(a_1) = 1.270 \pm 0.015 GeV$ and $\Gamma(a_1) = 0.604 \pm 0.050 GeV$ |
| $h^-h^+h^-\pi^0\nu$ | $4.25 \pm 0.13 \pm 0.13$ | ALEPH | 1989-92 | [68] | $\omega\pi$ fraction$= 0.450 \pm 0.019^{+0.025}_{-0.026}$ |
| | $4.25 \pm 0.09 \pm 0.26$ | CLEO | | [67] | |
| $3\pi^-2\pi^+\nu$ | $0.077 \pm 0.005 \pm 0.009$ | CLEO | | [69] | |
| $3\pi^-2\pi^+\pi^0\nu$ | $0.019 \pm 0.004 \pm 0.004$ | CLEO | | [69] | |
| $3\pi^-2\pi^+2\pi^0\nu$ | $< 0.011$ (90 % C. L.) | CLEO | | [69] | |

**Table 6.** Recent measurements of the tau branching fractions.

new results on the elements $V_{cb}$ and $V_{td}$.

### *3.1.* $V_{cb}$

*3.1.1. Inclusive b semileptonic decay.* There are several techniques for extracting $V_{cb}$; all use the semileptonic decays $b \to c\ell\nu$, where $\ell$ represents an $e$ or $\mu$. The first technique looks at the inclusive semileptonic rate, that is, the sum over all final states. To first order this process is free quark decay, and accordingly we write the rate as

$$\Gamma(b \to c\ell\nu) = \frac{\mathrm{B}(b \to c\ell\nu)}{\tau_b} = \frac{G_F^2 m_b^5}{192\pi^3}|V_{cb}|^2\kappa,$$

where $G_F$ is the weak coupling constant, $m_b$ is the $b$ quark mass, and the factor $\kappa$ accounts for phase space and corrections for the fact that the $b$ quark is not free, but bound into a meson or baryon. The value of $m_b$ is uncertain, as is the value of $\kappa$, thanks to non-perturbative QCD contributions. As we shall see below, uncertainties in the values of $\kappa$ and $m_b$ dominate uncertainty in the value of $V_{cb}$ determined from inclusive $b$ semileptonic decay.

Experimentally, we want to determine the $b \to c\ell\nu$ branching fraction and the $b$ lifetime. To measure the branching fraction, one isolates $b$ decays and then plots the momentum spectrum of all observed leptons. Unfortunately leptons originate not only from $b \to c\ell\nu$ decays but also from two other sources that must be subtracted as background. The first is $b \to u\ell\nu$, whose rate is about 1/70 that of $b \to c\ell\nu$ and is therefore easily corrected for. The second, much more important, background comes from secondary decays in which the $b$ decays hadronically, and the lepton comes from the decay of one of its daughters. At the $\Upsilon(4S)$, where $B$ mesons are produced nearly at rest, this background is suppressed by requiring that the lepton momentum be large, typically above 1.5 GeV/$c$, but with the price of increased model dependence since one must predict the fraction of the spectrum above this cut. At the $Z^0$ resonance the same problems arise as at the $\Upsilon(4S)$, but in addition, the fragmentation of the $b$ quark is uncertain and there are additional non-$b$ backgrounds.

CLEO has a new measurement of the $b \to ce\nu$ branching fraction [86] that circumvents the model dependence described above by using a technique first introduced by ARGUS [87]. First, events with two leptons are selected. The first lepton, which

| Mode | Branching fraction (%) | Expt. | Data sample | | Comments |
|---|---|---|---|---|---|
| $K^-\nu$ | $0.85 \pm 0.18$ | DELPHI | 1992 | [70] | |
| | $0.98 \pm 0.19 \pm 0.22$ | OPAL | 1990,91 | [71] | |
| | $0.64 \pm 0.05 \pm 0.05$ | ALEPH | 1991,92 | [72] | |
| | $0.66 \pm 0.07 \pm 0.09$ | CLEO | | [73] | |
| $K^-\nu \geq 0$ *neutrals* | $1.54 \pm 0.24$ | DELPHI | 1992 | [70] | |
| | $1.60 \pm 0.07 \pm 0.12$ | ALEPH | 1991,92 | [72] | $K^0$ treated as a neutral |
| | $1.60 \pm 0.012 \pm 0.19$ | CLEO | | [73] | |
| $K^-\nu \geq 1$ *neutral* | $0.69 \pm 0.25$ | DELPHI | 1992 | [70] | |
| $K^-\pi^0\nu$ | $0.51 \pm 0.10 \pm 0.07$ | CLEO | | [73] | |
| | $0.53 \pm 0.05 \pm 0.07$ | ALEPH | 1991,92 | [72] | |
| $h^-K^0\nu$ | $0.997 \pm 0.023 \pm 0.108$ | CLEO | | [74] | |
| | $1.28 \pm 0.16 \pm 0.12$ | ALEPH | 1991,92 | [75] | Uses $K_S$ |
| $\pi^-K^0\nu$ | $0.88 \pm 0.14 \pm 0.09$ | ALEPH | 1991,92 | [76] | Uses $K_L$ |
| $h^-K^0\nu \geq 0$ *neutrals* | $1.98 \pm 0.38$ | DELPHI | 1991,92 | [77] | Uses $K_S$ |
| | $2.34 \pm 0.18 \pm 0.12$ | ALEPH | 1991,92 | [75] | Uses $K_S$ |
| | $1.72 \pm 0.16 \pm 0.10$ | OPAL | 1990-92 | [78] | Uses $K_S \to \pi^+\pi^-$ |
| $K^{*-}\nu \geq 0h^0$ (*not* $\pi^0$ *or* $K_S$) | $1.73 \pm 0.24 \pm 0.13$ | OPAL | 1990-92 | [78] | Uses $K^* \to K_S\pi^-$ |
| | $1.19 \pm 0.15^{+0.12}_{-0.15}$ | ARGUS | | [79] | |
| $K^{*-}\nu$ | $1.71 \pm 0.72$ | DELPHI | 1992 | [70] | Uses $K^-\pi^0$ |
| | $1.74 \pm 0.42$ | DELPHI | 1991,92 | [77] | Uses $K_S\pi^-$ |
| | $1.46 \pm 0.12 \pm 0.09$ | ALEPH | 1991,92 | [75] | Combines all $K^*$ modes |
| | $0.97 \pm 0.15^{+0.11}_{-0.12}$ | ARGUS | | [79] | Supersedes their previous result |
| $K^-\pi^+\pi^-\nu$ | $0.33 \pm 0.11 \pm 0.13$ | ARGUS | | [79] | |
| | $0.58^{+0.15}_{-0.13} \pm 0.12$ | TPC | | [80] | They find mass distributions consistent with $K_1$ dominance. |
| $h^-K^0\pi^0\nu$ | $0.519 \pm 0.035 \pm 0.062$ | CLEO | | [74] | |
| $\pi^-\bar{K}^0\pi^0\nu$ | $0.33 \pm 0.14 \pm 0.07$ | ALEPH | 1991,92 | [76] | Uses $K_L$ |
| $K^-\pi^0\pi^0\nu$ | $< 0.3$ (90 % C.L.) | CLEO | | [73] | |
| | $0.04 \pm 0.03 \pm 0.02$ | ALEPH | 1991,92 | [72] | |
| $\pi^-K^+\pi^-\nu$ | $< 0.25$ (90% C.L.) | TPC | | [80] | |
| $\bar{K}^{*0}\pi^-\nu$ | $0.21 \pm 0.09 \pm 0.05$ | ARGUS | | [79] | |
| $K^-K^0\nu$ | $0.123 \pm 0.023 \pm 0.023$ | CLEO | | [81] | |
| | $0.28 \pm 0.12 \pm 0.03$ | ALEPH | 1991,92 | [76] | Uses $K_L$ |
| $K^-K^0\pi^0\nu$ | $0.129 \pm 0.050 \pm 0.032$ | CLEO | | [81] | |
| | $0.05 \pm 0.05 \pm 0.01$ | ALEPH | 1991,92 | [76] | Uses $K_L$ |
| $h^-K^0K^0\nu$ | $0.083 \pm 0.017 \pm 0.017$ | CLEO | | [82] | Uses $K_S$ |
| $K^-K^+\pi^-\nu$ | $< 0.17$ (95% C. L. ) | ARGUS | | [79] | |
| | $0.15^{+0.09}_{-0.07} \pm 0.03$ | TPC | | [80] | |
| $K^-\pi^+K^-\nu$ | $< 0.09$ (90% C.L.) | TPC | | [80] | |
| $K^-K^{*0}\pi^-\nu$ | $0.18 \pm 0.05 \pm 0.03$ | ARGUS | | [79] | |
| $K^-K^+K^-\nu$ | $< 0.21$ (90% C.L.) | TPC | | [80] | |

**Table 7.** Recent measurements of branching fractions of tau decays to final states with kaons.

| Mode | Result (%) | Expt. | Data sample | | Comments |
|---|---|---|---|---|---|
| $\tau \to 1 - prong$ | $85.09^{+0.15}_{-0.13} \pm 0.15$ | ALEPH | 1991,92 | [83] | B1+B3+B5=1 constraint |
| | $84.08 \pm 0.59 \pm 0.45$ | DELPHI | 1991 | [84] | Luminosity normaliztion |
| | $85.07 \pm 0.21 \pm 0.30$ | DELPHI | 1992 | [85] | B1+B3+B5=1 constraint |
| $\tau \to 3 - prong$ | $14.79^{+0.13}_{-0.15} \pm 0.16$ | ALEPH | 1991,92 | [83] | B1+B3+B5=1 constraint |
| | $15.00 \pm 0.37 \pm 0.21$ | DELPHI | 1991 | [84] | Luminosity normaliztion |
| | $14.60 \pm 0.22 \pm 0.30$ | DELPHI | 1992 | [85] | B1+B3+B5=1 constraint |
| $\tau \to 5 - prong$ | $0.097 \pm 0.005 \pm 0.011$ | CLEO | | [69] | |
| | $0.11^{+0.03}_{-0.02} \pm 0.02$ | ALEPH | | [83] | B1+B3+B5=1 constraint |
| | $0.31 \pm 0.11 \pm 0.07$ | DELPHI | 1991 | [84] | Luminosity normaliztion |
| | $0.33 \pm 0.11 \pm 0.10$ | DELPHI | 1992 | [85] | B1+B3+B5=1 constraint |

**Table 8.** Recent measurements of the tau topological branching fractions.

| Mode | World Average Branching Fraction (%) | Total |
|---|---|---|
| $e\nu\bar{\nu}$ | $17.66 \pm 0.11$ | |
| $\mu\nu\bar{\nu}$ | $17.18 \pm 0.12$ | |
| $h^-\nu$ | $12.03 \pm 0.20$ | |
| $h^-\pi^0\nu$ | $25.29 \pm 0.37$ | |
| $h^-\pi^0\pi^0\nu$ | $9.07 \pm 0.27$ | |
| $h^-\pi^0\pi^0\pi^0\nu$ | $1.20 \pm 0.13$ | $84.48 \pm 0.58$ |
| $h^-\pi^0\pi^0\pi^0\pi^0\nu$ | $0.16 \pm 0.07$ | |
| $h^-\pi^0\eta\nu, \eta \to \gamma\gamma$ | $0.07 \pm 0.01$ | |
| $h^-\omega\nu, \omega \to \pi^0\gamma$ | $0.18 \pm 0.02$ | |
| $h^-\omega\pi^0\nu, \omega \to \pi^0\gamma$ | $0.03 \pm 0.01$ | |
| $h^-K^0 n\pi^0\nu, n \geq 0$ | $1.61 \pm 0.16$ | |
| $\tau \to 1 - prong$ | $85.26 \pm 0.19$ | |
| $3h^-\nu$ | $8.91 \pm 0.34$ | |
| $3h^-\pi^0\nu$ | $4.25 \pm 0.15$ | $13.64 \pm 0.38$ |
| $3h^-\pi^0\pi^0\nu$ | $0.48 \pm 0.06$ | |
| $\tau \to 3 - prong$ | $14.64 \pm 0.19$ | |
| $5h^-\nu$ | $0.07 \pm 0.01$ | |
| $5h^-\pi^0\nu$ | $0.02 \pm 0.071$ | $0.09 \pm 0.01$ |
| $\tau \to 5 - prong$ | $0.10 \pm 0.01$ | |
| Sum of exclusive modes | | $98.2 \pm 0.7$ |

**Table 9.** Summary of the tau branching fractions.

serves as a tag, must have momentum greater than 1.4 GeV$/c$ so that it is known to come from $b \to c\ell\nu$ decay. The charge of the second lepton (an electron) then betrays its origin: if it is also from $b \to c\ell\nu$ decay then its charge is opposite that of the first lepton. On the other hand, if it is the product of a secondary decay from the other $B$ meson then the charges of the two leptons will match. Angular cuts suppress events in which both leptons come from the same $B$. Mixing of neutral $B$ mesons reverses the charge correlations for some events, but can be corrected for. The momentum spectrum of the second lepton in same sign and opposite sign events are shown in figure 7. The primary $b \to ce\nu$ distribution now extends down to 0.6 GeV$/c$, so the branching fraction is nearly model independent. They find $\mathrm{B}(b \to ce\nu) = (10.36 \pm 0.17 \pm 0.40)\%$.

Measurements of the inclusive $b \to c\ell\nu$ branching fraction at the $\Upsilon(4S)$ and $Z^0$ are summarized in table 10. There are two interesting things about the averages. First, they are lower than predicted by most theorists. This point is discussed in these proceedings by Roudeau [2]. Second, in contrast to theoretical predictions that the semileptonic widths of all the $b$ hadrons are the same at the current level of precision, the branching fractions measured at the $Z^0$ and $\Upsilon(4S)$ are in mild disagreement (2 standard deviations), suggesting that the systematic uncertainties of the lifetimes or some of the branching fractions may be underestimated. Because of this disparity, the LEP and $\Upsilon(4S)$ results are treated separately below.

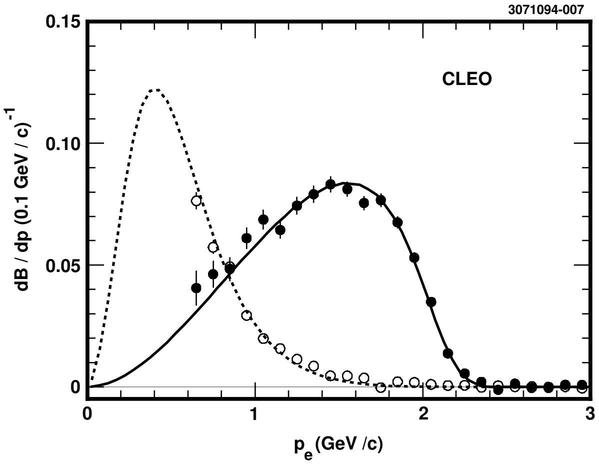


**Figure 7.** The momentum spectra of electrons from primary decays $B \to Xe\nu$ (filled circles) and secondary decays $b \to c \to ye\nu$ (open circles) from analysis of $B\bar{B}$ events tagged by a high-momentum lepton. The curves show the results of fits to the ACCMM model (CLEO).

To extract the value of $|V_{cb}|$, we combine these branching fractions with the lifetimes. We combine the $Z^0$ result with the average $b$ hadron lifetime measured at LEP, $(1.55 \pm 0.06)$ ps, and we combine the branching fraction measured at the $\Upsilon(4S)$ with the average of the $B^+$ and $B^0$ meson lifetimes of $(1.63 \pm 0.07)$ ps [2]. These then yield the values of $|V_{cb}|$:

$$\Upsilon(4S) \quad |V_{cb}| = \quad 0.039 \pm 0.001 \pm 0.005 \qquad (1)$$
$$Z^0 \quad |V_{cb}| = \quad 0.042 \pm 0.002 \pm 0.005, \qquad (2)$$

where the first error is experimental and the second

| | Expt. | Data Sample | | Result (%) | |
|---|---|---|---|---|---|
| $\Upsilon(4S)$ | CRYSTAL BALL | | [89] | $12.0 \pm 0.5 \pm 0.7$ | $1\ell$ |
| | ARGUS | | [90] | $10.2 \pm 0.5 \pm 0.2$ | $1\ell$ |
| | CUSB | | [91] | $10.0 \pm 0.4 \pm 0.3$ | $1\ell$ |
| | CLEO | | [92] | $10.5 \pm 0.2 \pm 0.4$ | $1\ell$ |
| | CLEO | | [93] | $10.48 \pm 0.07 \pm 0.33$ | $1\ell$ |
| | ARGUS | | [87] | $9.7 \pm 0.5 \pm 0.4$ | $2\ell$ |
| | CLEO | | [86] | $10.36 \pm 0.17 \pm 0.40$ | $2\ell$ |
| | | $\Upsilon(4S)$ Average | | $10.31 \pm 0.10 \pm 0.25$ | |
| $Z^0$ | L3 | 90,91 | [94] | $11.73 \pm 0.48 \pm 0.28 \pm 0.31$ | |
| | OPAL | 90,91 | [95] | $10.5 \pm 0.6 \pm 0.4 \pm 0.4$ | |
| | ALEPH | 90,91 | [94] | $11.40 \pm 0.33 \pm 0.37 \pm 0.20$ | |
| | DELPHI | 91,92 | [96] | $11.41 \pm 0.45 \pm 0.50 \pm 0.31$ | |
| | | $Z^0$ Average | | $11.33 \pm 0.22 \pm 0.41$ | |

**Table 10.** Experimental values of the inclusive branching fraction $b \to c\ell\nu$. For the $\Upsilon(4S)$ results the value quoted uses the ACCMM model [88], chosen to facilitate comparison with the LEP results, most of which also use this model. In combining the results, an additional common systematic error of 0.3% was assigned to the measurements made using the single lepton technique at the $\Upsilon(4S)$ to account for the model dependence and a common systematic uncertainty of 0.1% was assumed for the dilepton results. For the LEP experiments the model dependence appears as the third error; in combining them a common error of 0.4% was assumed.

is the theoretical uncertainty arising from the factor $m_b^5\kappa$ and covers the central values of models due to Bigi and Uraltsev [97], Shifman *et al.*[98], Ball and Nierste [99] and Luke and Savage [100].

The L3 experiment reported a measurement of the $b$ semileptonic branching fraction using a very different technique [101]. They use the fact that the visible energy in the hemisphere associated with $b$ quark decay is small if one or more neutrinos is present. Based on the distribution of visible energy, they find a total semileptonic branching fraction of $(22.7 \pm 0.8 \pm 1.5)\%$. To compare this with the measurements $\mathrm{B}(b \to c\ell\nu)$, we subtract $(2.98 \pm 0.47)\%$ for the contribution from $b \to c\tau\nu$ (see section 4.0.4) and divide by two. This yields $b \to c\ell\nu = (9.9 \pm 0.9)\%$, consistent with both the $\Upsilon(4S)$ and the $Z^0$ results found above.

*3.1.2. $B \to D^*\ell\nu$.* We next turn to the decay $B \to D^*\ell\nu$. We will take some time to develop the theory of this decay since there are several important results relevant to it. In a simple picture, we view the $B$ meson as the bound state of $b$ and $u$ quarks. Let us consider the recoil of the $c$ quark produced when the $b$ quark decays, assuming that both quarks have infinite mass. At one kinematic extreme, the lepton and the neutrino emerge back-to-back, and the $c$ quark remains at rest. From the standpoint of the meson little has happened (aside from a change of identity!). If we define $q^2$ as the invariant mass squared of the virtual $W$ mediating the decay, then $q^2$ is maximized in this configuration. At the opposite extreme, for which $q^2 = q^2_{min}$, the lepton and the neutrino emerge in the same direction. In this case the $c$ quark recoils rapidly against them; in order for a $D$ or $D^*$ meson to form, the $u$ quark must "keep up" with the $c$ quark. This necessity suppresses the rate for this configuration.

In the heavy quark limit this suppression is parametrized by the Isgur-Wise function, $\xi(q^2)$. Though the detailed shape of the Isgur-Wise is unknown, its general features are clear from the description above. First, its value is unity at $q^2 = q^2_{max}$; we will exploit this feature to extract $|V_{cb}|$. As $q^2$ decreases, the Isgur-Wise function falls, and the additional belief that form factors should remain positive at all values of $q^2$ implies that $\xi(q^2)$ has mild positive curvature. In what follows, it will be parametrized as a linear function of $q^2$.

At this juncture it is convenient to define a new variable,

$$w = v_B \cdot v_{D^*} = \frac{m_B^2 + m_{D^*}^2 - q^2}{2m_B m_{D^*}}.$$

In the $B$ meson rest frame, $w = E_{D^*}/m_{D^*}$. At $q^2_{max}$ $w = 1$, while at $q^2_{min}$, $w \approx 1.5$. In terms of this variable, we have

$$\xi(1) = 1 \tag{3}$$

and

$$\xi(w) = 1 - \rho^2(1-w) \quad . \tag{4}$$

This picture changes somewhat when one accounts for the finite masses of the $b$ and $c$ quarks. First, instead of a single function parametrizing the quark overlap, there are now four form factors;

their earlier degeneracy was a consequence of the symmetry in the quark masses and this now evaporates. In addition, the Isgur-Wise function $\xi(w)$ becomes $\hat{\xi}(w)$ (the "hat" ( $\hat{}$ ) distinguishes the physically observable quantities from those that apply only in the heavy quark limit), and the value of $\hat{\xi}(1)$ is shifted from unity. First order corrections to $\hat{\xi}(1)$ vanish by Luke's theorem [102]; however, there are significant higher order corrections, and uncertainty in these will appear as an uncertainty in the value of $V_{cb}$.

To quantify the splitting of the form factors, we introduce the ratios

$$R_1 = \left[1 - \frac{q^2}{(m_B+m_{D^*})^2}\right]^{-1} \frac{V(q^2)}{A_1(q^2)}$$

$$R_2 = \left[1 - \frac{q^2}{(m_B+m_{D^*})^2}\right]^{-1} \frac{A_2(q^2)}{A_1(q^2)}.$$

where $A_1(q^2)$, $V(q^2)$ and $A_2(q^2)$ are the traditional $B \to D^*\ell\nu$ form factors, whose relationships to the Isgur-Wise function are summarized in table 11. In the heavy quark limit, $R_1 = R_2 = 1$. Neubert has calculated both the first order corrections in $\Lambda_{QCD}/m_B$ and the short distance corrections to $R_1$ and $R_2$ [103][104], yielding the predictions $R_1 = 1.3\pm0.1$ and $R_2 = 0.8\pm0.1$, with a weak dependence on $w$.

CLEO has presented a new analysis of $B \to D^*\ell\nu$ form factors. They use the distributions of the kinematic variables $q^2$, $\cos\theta_\ell$, $\cos\theta_V$ and $\chi$, defined in figure 8 to extract the values of $\rho^2$ (here defined as the slope of the hadronic form factor $h_{A_1}$), $R_1$ and $R_2$ using a 4-dimensional unbinned maximum likelihood fit. They assume a linear form for the Isgur-Wise function and that $R_1$ and $R_2$ are independent of $w$. This analysis is the first to allow all of these parameters to vary simultaneously, and it is the most precise to date. Projections of the fit are shown in figure 9. The results are

$$\begin{aligned} R_1 &= 1.30 \pm 0.36 \pm 0.16 \\ R_2 &= 0.64 \pm 0.26 \pm 0.12 \\ \rho^2 &= 1.01 \pm 0.15 \pm 0.09. \end{aligned} \quad (5)$$

The values of these three parameters are correlated with one another, with the coefficients

$$\begin{aligned} C(R_1, R_2) &= -0.83 \\ C(R_1, \rho^2) &= 0.63 \\ C(R_2, \rho^2) &= -0.82. \end{aligned} \quad (6)$$

These results are compatible with the predictions of the heavy quark theory, though they are not yet precise enough to discern the $\Lambda/m_B$ corrections from the heavy quark limit. Consistency of these results with the predictions of HQET adds confidence to the value of $V_{cb}$ obtained by exploiting HQET.

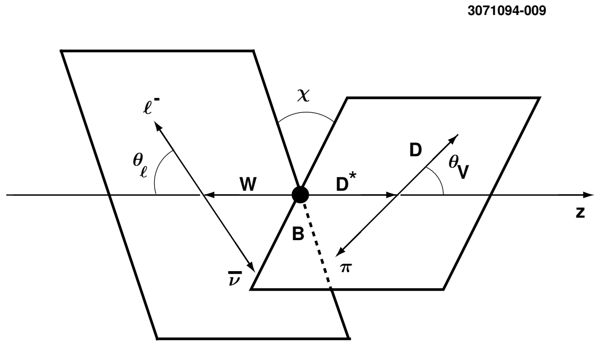


**Figure 8.** The kinematic variables used to extract the $B \to D^*\ell\nu$ form factors. The angles $\theta_\ell$ and $\theta_V$ are calculated in the rest frames of the virtual $W$ and the $D^*$ respectively.

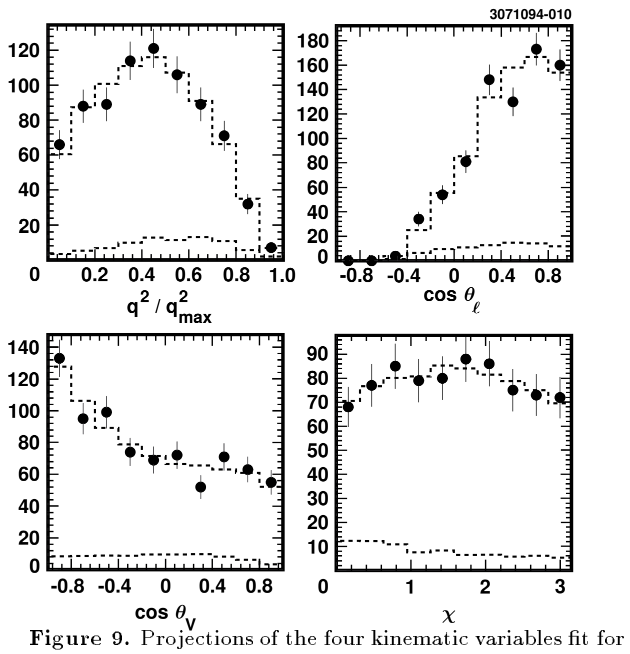


**Figure 9.** Projections of the four kinematic variables fit for the $B \to D^*\ell\nu$ form factors for the data (closed circles), the fit (upper dashed line) and the background (lower dashed line)(CLEO).

We turn now to the extraction of $|V_{cb}|$ from $B \to D^*\ell\nu$ decays. The CLEO collaboration reconstructs both the $B^0 \to D^{*+}\ell^-\nu$ and $B^- \to D^{*0}\ell^-\nu$ decays [105]. In the former case, they require that $D^{*+} \to D^0\pi^+$ and in the latter, $D^{*0} \to D^0\pi^0$; in both cases the $D^0$ must decay to $K^-\pi^+$. The invariant mass distribution of $K^-\pi^+$ combinations in events satisfying all other selection criteria is shown in figure 10. They plot the distribution of these events as a function of $\tilde{w}$, where $\tilde{w}$ is $w$

| | | | |
|---|---|---|---|
| $B \to D\ell\nu$ | $F_1(q^2)$ | | $\xi(w)$ |
| $B \to D^*\ell\nu$ | $A_1(q^2)$ | $\left[1-\frac{q^2}{(m_B+m_{D^*})^2}\right]^{-1}$ | $\xi(w)$ |
| | $V(q^2)$ | | $\xi(w)$ |
| | $A_2(q^2)$ | | $\xi(w)$ |

**Table 11.** Form factors describing the decays $B \to D\ell\nu$ and $B \to D^*\ell\nu$ and their relation to the Isgur-Wise function.

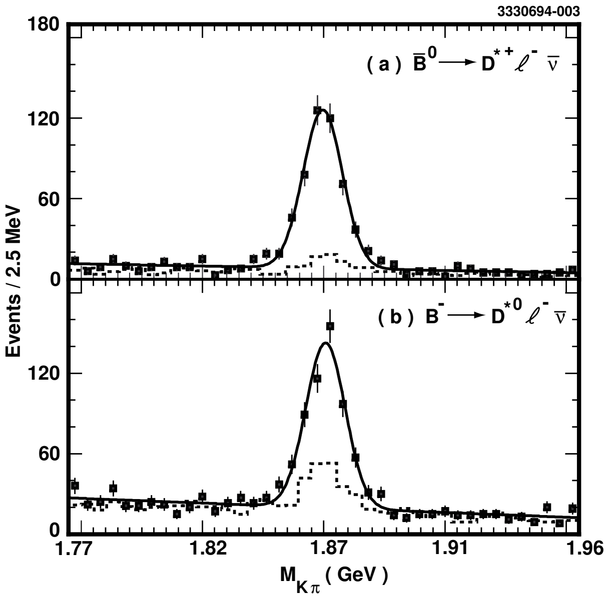


**Figure 10.** The invariant mass of $K^-\pi^+$ combinations satisfying all other selection criteria from (a) $\bar{B}^0 \to D^{*+}\ell^-\bar{\nu}$ and (b) $B^- \to D^{*0}\ell^-\bar{\nu}$. The dashed histograms show the background distribution and the solid lines show the fits used to determine the yield (CLEO).

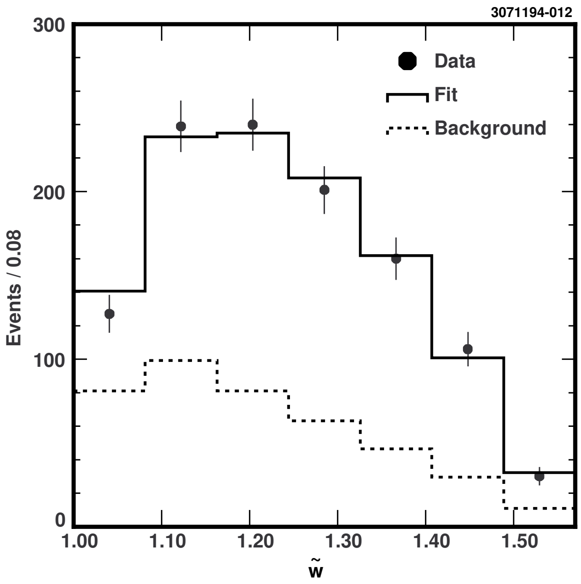


**Figure 11.** The $\tilde{w}$ distribution of $B \to D^*\ell\nu$ decays, for the data (filled circles), the fit (histogram) and the background (dashed histogram) (CLEO).

smeared by lack of knowledge of the direction of motion of the $B$. The shape of this distribution is determined by the Isgur-Wise function, phase space, and acceptance; its intercept at $w = 1$ determines the product $\hat{\xi}(1)\eta_A|V_{cb}|$, where $\eta_A$ is a QCD correction. The data are shown in figure 11 with the result of the fit superimposed, where the fit has accounted for the smearing between $w$ and $\tilde{w}$. The fit yields the slope $\hat{\rho}^2 = 0.84\pm0.13\pm0.08$, which agrees well with the value of $\rho^2$ found above after accounting for the assumption used in the fit that $R_1 = R_2 = 1$ [103]. The fit also yields the intercept $\hat{\xi}(1)\eta_A|V_{cb}| = 0.0347\pm0.0019(stat.)\pm0.0018(syst.)\pm 0.0008(lifetime)$, where we have used the values $\tau_{B^0} = (1.61\pm0.08)$ ps and $\tau_{B^-} = (1.65\pm0.07)$ ps [2]. In order to view the Isgur-Wise function directly, one can factor out phase space and acceptance. This is done in figure 12, where the horizontal axis displays the mean value of $w$ in each bin of $\tilde{w}$.

The ALEPH collaboration has done a similar analysis [106]; this is the first such analysis from LEP. Because of the large boost of the $B$ meson at LEP, this measurement has the advantage that the acceptance is good at all values of $q^2$ (this is in contrast to the $\Upsilon(4S)$ experiments, which have low efficiency to reconstruct the soft pion from $D^{*-} \to \bar{D}^0\pi^-$ decay near $q^2_{max}$); the drawback is that lack of knowledge of the (large) $B$ momentum makes it tricky to calculate the $q^2$ of the decay. To do it they use the flight direction of the $B$, which is taken to lie along the line from the interaction point to the decay vertex, and the neutrino energy, which is taken to be difference between the beam energy and the energy detected in the hemisphere containing the $B$ with corrections intended to account for three jet events. They reconstruct the decay chain $B^0 \to D^{*+}\ell^-\nu$ followed by $D^{*+} \to D^0\pi^+$ and $D^0 \to K^-\pi^+$ or $K^-\pi^+\pi^-\pi^+$ or $K_S\pi^-\pi^+$. The $q^2$ distribution of their data is shown in figure 13 with the fit superimposed. Assuming a linear form for the Isgur-Wise function, they find a slope of $\hat{\rho}^2 = 0.46\pm0.30\pm0.15$, consistent with the value found by CLEO, and $\hat{\xi}(1)\eta_A|V_{cb}| = 0.0364 \pm 0.0042(stat.) \pm 0.0029(syst.) \pm 0.0010(lifetime)$.

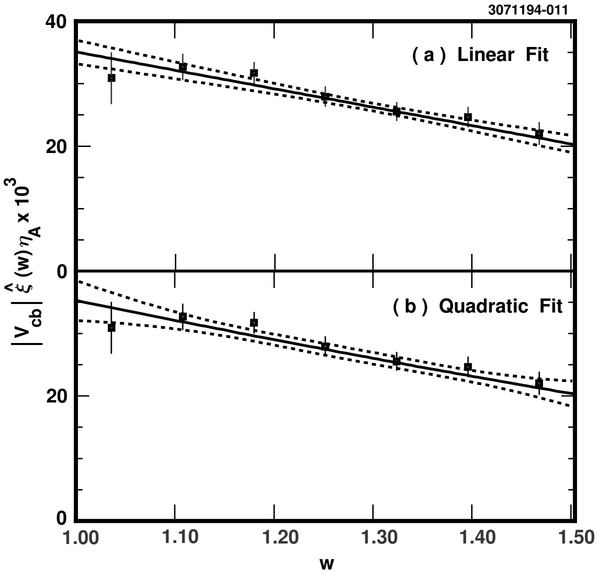


**Figure 12.** The value of $\hat{\xi}(w)\eta_A|V_{cb}|$ as a function of the mean value of $w$ in each bin of $\tilde{w}$ for $B \to D^*\ell\nu$ decays. The curve is the result of the fit of the data assuming (a) a linear function and (b) a quadratic function of $w$ (CLEO).

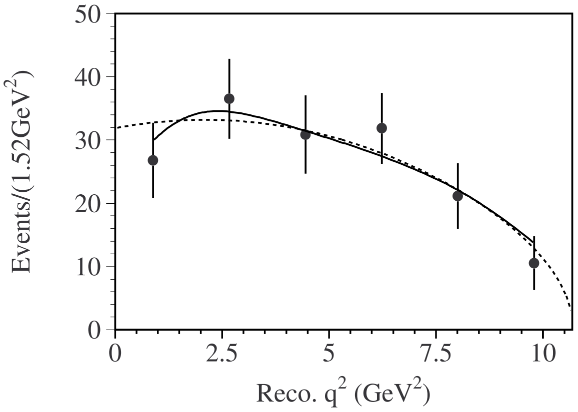


**Figure 13.** The $q^2$ distribution of $\bar{B}^0 \to D^{*+}\ell^-\bar{\nu}$ decays from ALEPH after background subtraction. The solid curve is the result of a fit, assuming a linear form for the Isgur-Wise function, and the dashed curve is the fitted function without including resolution effects.

Extraction of $|V_{cb}|$ from these measurements requires values for the parameters $\hat{\xi}(1)$ and $\eta_A$. The value of $\eta_A$ is calculable perturbatively within QCD, and here we will use $\eta_A = 0.985 \pm 0.015$ [104]. The value of $\hat{\xi}(1)$ is less certain. Neubert finds [104] $\hat{\xi}(1) = 0.945 \pm 0.025$, while Shifman *et al.* find [98] $\hat{\xi}(1) = 0.91 \pm 0.03$. Here we take a value that is compatible with both of these, $\hat{\xi}(1) = 0.93 \pm 0.04$. Additional uncertainty arises from uncertainty in the shape of the Isgur-Wise function: allowing a positive curvature in the fit rather than assuming a linear form increases the intercept at $w = 1$. Fits with various models by the CLEO collaboration are summarized in table 12. These indicate that the curvature is likely to shift the value of $V_{cb}$ by $+(0.001 \pm 0.001)$, so the following results have been corrected by this amount. The net theoretical uncertainty is $\pm 0.002$ on $V_{cb}$. The resulting values of $V_{cb}$ extracted from the experiments are summarized in table 13. Combining them yields the value

$$|V_{cb}| = 0.0400 \pm 0.0025 \pm 0.0020,$$

where the first error is the combined statistical and systematic error from the experiments, and the second is the systematic uncertainty due to the theory. This value of $|V_{cb}|$ is currently more precise than the value extracted from the inclusive lepton spectrum.

### *3.2. $V_{td}$*

Because the current world sample of top quarks is tiny, information about the CKM matrix element $V_{td}$ comes not from observations of top decays but from the short-lived existence of the top quarks in loops. The most precise determination of $V_{td}$ currently comes from $B\bar{B}$ mixing, which is discussed by Forty [1] in these proceedings. Other probes of $V_{td}$ that could prove useful in the future are the decays $B \to \rho\gamma$, $B \to \omega\gamma$, and $K \to \pi^+\nu\bar{\nu}$.

*3.2.1. $B \to \rho\gamma$ and $B \to \omega\gamma$.* The decay $B \to \rho\gamma$ is expected to occur in the standard model through a penguin diagram as shown in figure 14. The theoretical prediction for this rate is sensitive to the hadronization of the $u$ quark. Much of this uncertainty cancels, however, in the ratio of rates $\Gamma(B \to \rho(\omega)\gamma)/\Gamma(B \to K^*\gamma)$. Theoretical predictions of the short distance contributions are summarized in table 14. Long distance contributions may also be important; for example, Atwood *et al.* estimate [110] that the long distance amplitudes are at least 15 % as large as the short distance amplitudes. Studies of the related decays $B \to \rho\rho$, $B \to K^*\gamma$, $B \to \phi\gamma$ and measurement of the $B^- \to \rho^-\gamma$, $B^0 \to \rho^0\gamma$ and $B^0 \to \omega\gamma$ branching fractions should be sufficient to separate the short and long distance contributions.

CLEO has searched for the modes $B \to \rho\gamma$ and $B \to \omega\gamma$ [111]. The invariant mass distribution of their $\rho\gamma$ and $\omega\gamma$ candidates is shown in figure 15. After taking care to suppress background to the $B^0 \to \rho^0\gamma$ mode from $B^0 \to K^*\gamma$, the background is dominated by continuum processes. Assuming that all events arise from signal they find an upper limit

| Model | $\eta_A\hat{\xi}(1)\lvert V_{cb}\rvert$ |
|---|---|
| Linear | $0.0347 \pm 0.0019$ |
| Quadratic | $0.0349 \pm 0.0032$ |
| BSW [108] | $0.0365 \pm 0.0024$ |
| Pole | $0.0362 \pm 0.0024$ |
| ISGW [109] | $0.0357 \pm 0.0023$ |

**Table 12.** Results of the fit to $\eta_A\hat{\xi}(w)|V_{cb}|$ extrapolated to $w = 1$ for various form factors.

| Expt. | | $\lvert V_{cb}\rvert$ |
|---|---|---|
| ARGUS | [107] | $0.0430 \pm 0.0047 \pm 0.0030 \pm 0.002$ |
| CLEO | [105] | $0.0389 \pm 0.0021 \pm 0.0022 \pm 0.002$ |
| ALEPH | [106] | $0.0407 \pm 0.0046 \pm 0.0034 \pm 0.002$ |

**Table 13.** The values of $V_{cb}$ extracted from the $B \to D^*\ell\nu$ decay rate at zero recoil. The first error quoted is statistical, the second is systematic and includes uncertainty in the $B$ lifetime, and the third is a common error due to theory.

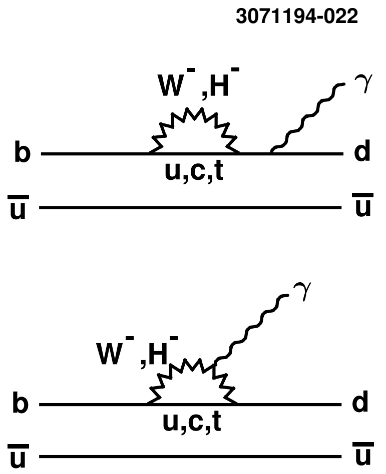


**Figure 14.** Penguin diagrams contributing to $B \to \rho(\omega)\gamma$.

of

$$\frac{\mathbf{B}(B \to \rho(\omega)\gamma)}{\mathbf{B}(B \to K^*\gamma)} < 0.34 \ (90\%\mathrm{C.L.}).$$

Neglecting the possibility of long distance contributions, this limit corresponds to the limit $|V_{td}/V_{ts}| < 0.64 - 0.76$ where the range depends on which theoretical calculation is used. This limit on $|V_{td}|$ is about a factor of two looser than constraints based on measurements of other CKM matrix elements and on the assumption that the matrix is unitary; however, in five to ten years these modes may provide an important test of $V_{td}$ .

*3.2.2.* $K^- \to \pi^-\nu\bar{\nu}$*.* A second promising channel is $K^- \to \pi^-\nu\bar{\nu}$. For this mode the theoretical uncertainty is small compared to other channels

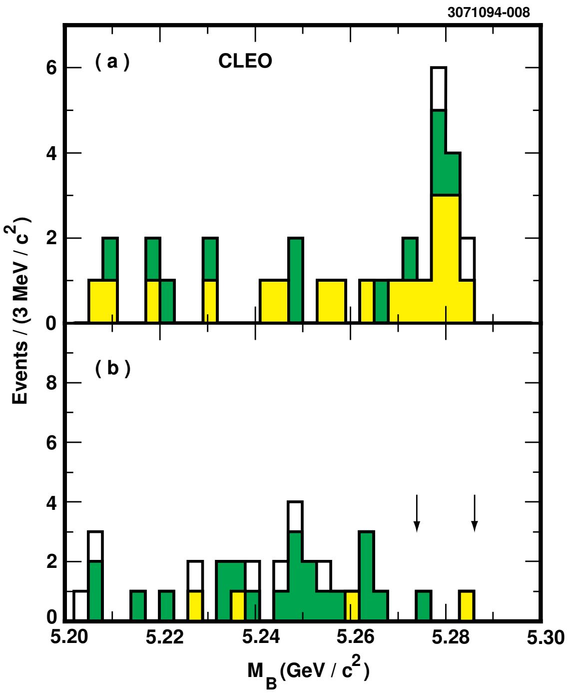


**Figure 15.** The invariant mass distribution of (a) $B \to K^*\gamma$ and (b) $B \to \rho(\omega)\gamma$ candidates based on samples of 1.4 fb$^{-1}$ and 2.0 fb$^{-1}$ respectively. The arrows indicate the signal region, $5.274 < M_B < 5.286$ GeV/$c^2$. The light gray entries are $K^-\pi^+\gamma(\rho^0\gamma)$ candidates, the dark gray $K^-\pi^0\gamma(\rho^-\gamma)$, and the white $K_S\pi^-\gamma(\omega\gamma)$ (CLEO).

sensitive to $V_{td}$: long distance effects are small and the hadronic matrix element can be determined using the related decay $K^- \to \pi^0e^-\bar{\nu}$. The dominant uncertainty comes from QCD corrections, which have been calculated by Buchalla and Buras [115] and are known within about $\pm 7\%$. Unfortunately the expected branching fraction is

| Model | $f$ | Ref. |
|---|---|---|
| QCD Sum Rules | 0.58 | Ali, *et al.* [112] |
| BSW Formalism | 0.81 | Soares [113] |
| Hybrid QCD Sum Rules | 0.77 | Narison [114] |

**Table 14.** Hadronic corrections to $\Gamma(B \to \rho(\omega)\gamma)/\Gamma(B \to K^*\gamma)$.

small, in the range 0.5 to $3 \times 10^{-10}$. The E787 collaboration at the AGS has searched for this mode, and new results were reported at this conference [116]. They stop kaons in a target and reconstruct the single emerging track. The principle backgrounds are $K^- \to \pi^-\pi^0$ and $K^- \to \mu^-\nu$. Three characteristics distinguish the signal. First, the charged particles produced in the two-body $\pi^\pm\pi^0$ and $\mu\nu$ decays are monoenergetic and can therefore be suppressed with suitable energy cuts; here the $\pi^-$ energy is required to lie between the energies of these two backgrounds. Second, the $\pi^-$ in signal events would have a characteristic range in an instrumented absorber called the "range stack". Third, the time sequence of the entire decay chain

$$\begin{array}{l} K^- \to \pi^-\nu\bar{\nu} \\ \qquad \hookrightarrow \mu^-\nu \\ \qquad\quad \hookrightarrow e^-\nu\bar{\nu} \end{array}$$

can be reconstructed using TDC's instrumenting the range stack and target. Their results from the 1989-91 data sample are shown in figure 16. They see no events in the signal box, and find a limit of $B(K^- \to \pi^-\nu\bar{\nu}) < 3.7 \times 10^{-9}$ (90% C.L.). Combining this with their previous result based on events in which the $\pi^-$ energy is below that of the $\pi^-$ from $\pi^\pm\pi^0$ decay [117], yields a new limit of $B(K^- \to \pi^-\nu\bar{\nu}) < 3.0 \times 10^{-9}$ (90% C.L.). This collaboration has recently upgraded their detector and beam line and have started a new run with an expected single event sensitivity of about $10^{-10}$, comparable to the expected rate for this decay.

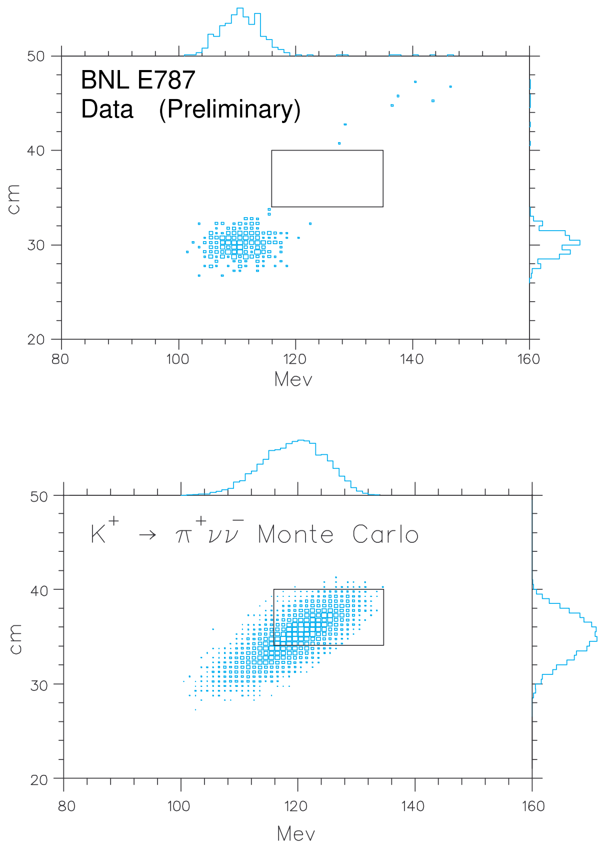


**Figure 16.** The distribution of the range of the candidate pion versus its kinetic energy for the data (upper plot) and Monte Carlo simulated signal (lower plot). No $K^- \to \pi^-\nu\bar{\nu}$ candidates are observed (BNL E787).

## 4. Searches for New Physics

Searches for new physics include direct searches for new particles, searches for rates which could be shifted by the presence of virtual new particles, and searches for violations of normally conserved quantities, such as lepton number. The first of these topics is covered in Reference [118].

*4.0.3. Searches for Lepton Number Violation.* Lepton number differs from other familiar conservation laws in that there is no known symmetry associated with it. As a result it need not be conserved, and indeed lepton number is violated in many extensions to the standard model such as supersymmetric models, extended technicolor and models that include right-handed neutrinos or leptoquarks. The predictions for lepton number violation are as wide ranging as the models themselves. For example, the decay $K_L \to \mu e$ provides the strongest bound on leptoquarks (the current limit bounds the mass of leptoquarks at 90 TeV if leptoquarks have standard weak couplings to fermions) [119], while $\mu \to e\gamma$ provides the strongest limit for certain other models, and $\tau \to \mu\gamma$ is most important for still others [120]. The current limits on lepton flavor violating modes are summarized in table 15.

One of the most precise searches numerically comes from SINDRUM II [125]. They look for muon to electron conversion through the exchange of a new particle with one of the nucleons in a titanium target. Because this is an elastic process, the amplitudes from all nucleons would add coherently, leading to a very sensitive probe. The momentum

| Mode | Upper Limit | C.L. | Collaboration | | |
|---|---|---|---|---|---|
| $\mu \to e\gamma$ | $4.9 \times 10^{-11}$ | 90% | MEGA | 1988 | [121] |
| $\tau \to \mu\gamma$ | $4.2 \times 10^{-6}$ | 90% | CLEO | 1993 | [122] |
| $\mu \to eee$ | $1.0 \times 10^{-12}$ | 90% | SINDRUM | 1988 | [123] |
| $\tau \to eee$ | $3.3 \times 10^{-6}$ | 90% | CLEO | 1994 | [124] |
| $\tau \to \mu ee$ | $3.4 \times 10^{-6}$ | 90% | CLEO | 1994 | [124] |
| $\tau \to e\mu\mu$ | $3.6 \times 10^{-6}$ | 90% | CLEO | 1994 | [124] |
| $\tau \to \mu\mu\mu$ | $4.3 \times 10^{-6}$ | 90% | CLEO | 1994 | [124] |
| $\mu + N \to e + N$ | $1.0 \times 10^{-12}$ | 90% | SINDRUM II | 1993 | [125] |
| $\mu^+ e^- \to \mu^- e^+$ | $6.5 \times 10^{-7}$ | 90% | LAMPF, Matthias *et al.* | 1991 | [126] |
| $\pi^0 \to \mu e$ | $8.6 \times 10^{-9}$ | 90% | FNAL E799 | 1994 | [127] |
| $K_L \to \mu e$ | $3.3 \times 10^{-11}$ | 90% | BNL E791 | 1993 | [128] |
| $D^0 \to \mu e$ | $1.0 \times 10^{-4}$ | 90% | ARGUS | 1988 | [129] |
| $B^0 \to \mu e$ | $5.9 \times 10^{-6}$ | 90% | CLEO | 1994 | [130] |
| $B^0 \to \tau e$ | $5.3 \times 10^{-4}$ | 90% | CLEO | 1994 | [130] |
| $B^0 \to \tau\mu$ | $8.3 \times 10^{-4}$ | 90% | CLEO | 1994 | [130] |
| $K^+ \to \pi^+ \mu e$ | $2.1 \times 10^{-10}$ | 90% | BNL E777 | 1990 | [131] |
| $B^+ \to K^+ \mu e$ | $1.2 \times 10^{-5}$ | 90% | CLEO | 1994 | [132] |
| $B^0 \to K^{*0} \mu e$ | $2.7 \times 10^{-5}$ | 90% | CLEO | 1994 | [132] |
| $Z^0 \to e\mu$ | $0.6 \times 10^{-5}$ | 95% | L3 | 1993 | [133] |
| $Z^0 \to e\tau$ | $8.7 \times 10^{-6}$ | 95% | L3 | 1994 | [134] |
| $Z^0 \to \mu\tau$ | $1.1 \times 10^{-5}$ | 95% | L3 | 1994 | [134] |

**Table 15.** Limits on lepton number violation.

spectrum of electrons emerging from their target is shown in figure 17. The spectrum is dominated by $\mu \to e\nu\bar{\nu}$ decay of captured muons. An electron emerging from $\mu e$ conversion would have a momentum above 100 MeV$/c$. They see no evidence for a signal, leading to a limit on the total rate for $\mu^- \to e^+$ conversion of

$$\Gamma(\mu^-\mathrm{Ti} \to e^-\mathrm{Ti})/\Gamma(\mu^-\mathrm{Ti\ capture}) < 1 \times 10^{-12}$$

with 90% confidence.

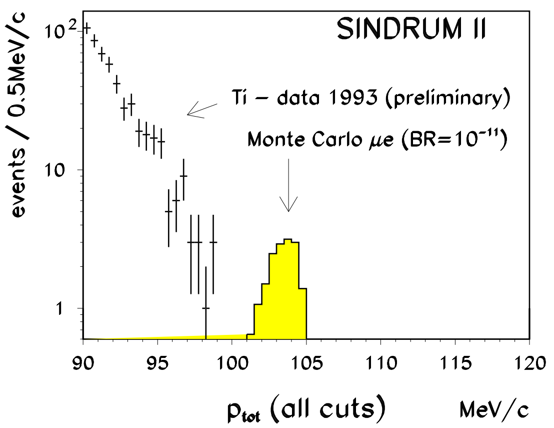


**Figure 17.** Measured electron momentum spectrum for the SINDRUM II data taken in 1993. A Monte Carlo simulation of the $\mu - e$ signal with an assumed branching fraction of B $= 10^{-11}$ is superimposed (shaded histogram).

*4.0.4. Searches for Charged Higgs Particles.* Charged Higgs' particles arise in many extensions to the standard model. In one class of models (including minimal supersymmetric models), there are two Higgs doublets, one of which gives mass to the $u$-type quarks and the other of which gives mass to the $d$-type quarks and charged leptons. Such Higgs' could take the place of $W$'s in familiar decays, and thereby shift the rate from the value predicted by the standard model. Decay modes whose rates are consistent with the standard model prediction therefore restrict the allowed values of the Higgs mass, $M_H$, and the ratio of vacuum expectation values of the two Higgs doublets, $\tan\beta$.

One sensitive decay is $B \to \tau\bar{\nu}X$. Two standard model predictions are $\mathbf{B}(b \to \tau\nu X)/\mathbf{B}(b \to e\nu X) = 0.26 \pm 0.03$ (Ref. [135]) and $0.22 \pm 0.02$ (Ref. [136]), corresponding to branching fractions of $(2-3)$ %. The most precise measurement of this mode comes from the ALEPH collaboration [137]. They use the fact that these decays have multiple neutrinos in the final state, and look for events with very large missing energy in one hemisphere. As shown in figure 18, they see a significant excess of such events, leading to the result $\mathbf{B}(b \to \tau\nu X) = (3.12 \pm 0.36 \pm 0.38)\%$. The L3 collaboration also looks for events with large missing energy [138] to find

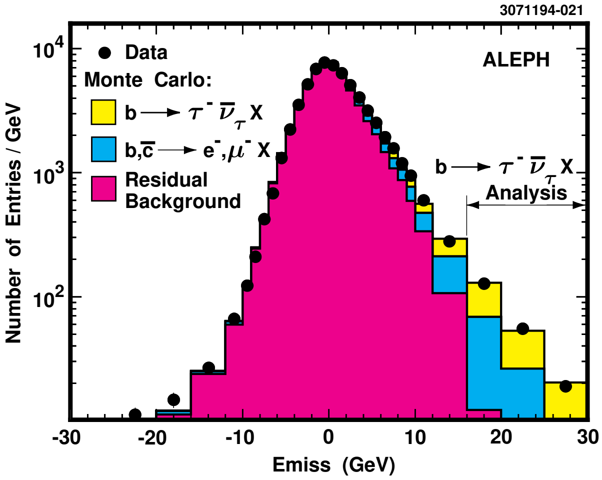


**Figure 18.** The distribution of the missing energy of one hemisphere for $b\bar{b}$ tagged events. Hemispheres containing identified leptons are excluded (ALEPH).

$\mathbf{B}(b \to \tau\nu X) = (2.4 \pm 0.7 \pm 0.8)\%$. The average of the two is $(2.98 \pm 0.47)\%$, which is consistent with the standard model predictions, and rules out charged Higgs particles with $M_H > (2.0GeV)\tan\beta$.

A related decay is $B \to \tau\nu$. In this decay, the $b$ and $u$ quarks of the $B$ meson annihilate and the virtual $W$ decays into the purely leptonic final state. This mode is of interest in the standard model in addition to limits on the Higgs because a measurement would provide clean information on the product $|V_{ub}|^2 f_B^2$, where $f_B$ is the $B$ meson decay constant, which currently limits the knowledge of $V_{td}$ from $B\bar{B}$ mixing measurements. There are two hitches: first, the expected branching fraction is low, of order $10^{-5}$ (because they are helicity suppressed the rates for $B \to \mu\nu$ and $B \to e\nu$ are even lower), and second, the multiple neutrinos in the final state leave few handles to distinguish these decays from background. The most precise limit to date comes from ALEPH [137], who use the same missing energy distribution that gave them the $B \to X\tau\bar{\nu}$ branching fraction, but this time looking in the range $E_{miss} > 35$ GeV (see figure 18). They see one event, consistent with the expected background level. Limits on this decay mode are summarized in table 16. They do not yet approach the standard model prediction; however, they do provide the constraint $M_H > (1.4\ GeV)\tan\beta \times (\frac{f_B|V_{ub}|}{0.75MeV})^{\frac{1}{2}}$, comparable to that provided by $B \to X\tau\nu$.

Finally we report on the first measurement of the branching fraction of the inclusive decay $b \to s\gamma$ [141]. Observation of the exclusive decay mode $B \to K^*\gamma$ last year [142] provided the first compelling evidence for penguin decays. Like the modes described above, the rate could be enhanced by a Higgs particle in place of the virtual $W$; however, uncertainty in the fraction of $b \to s\gamma$ decays that hadronize into $B \to K^*\gamma$ weakened the limit placed on the Higgs. The branching fraction of the inclusive mode $b \to s\gamma$ is much more readily interpreted. Observation of this mode was reported at this conference by the CLEO collaboration. At the $\Upsilon(4S)$, the photon produced is nearly monoenergetic, though the momentum of the $B$ meson (about 325 MeV/$c$), fermi motion of the $b$ quark within the meson, and gluon bremsstrahlung smear it somewhat. They require that the photon have an energy in the range $2.2 < E_\gamma < 2.7$ GeV. They then use two strategies to suppress background from events in which the photon comes from initial state radiation or an $e^+e^- \to q\bar{q}$ event. First, they loosely reconstruct the strange system recoiling against the photon. The resulting photon distribution is shown in figure 19. There is also evidence for a higher mass component. This analysis yields a branching fraction of $\mathrm{B}(b \to s\gamma) = (2.76 \pm 0.63) \times 10^{-4}$, where the error is statistical only. In their second approach, they use a neural net of kinematic variables to suppress the backgrounds. This approach leads to the photon energy spectrum shown in figure 20, and the branching fraction of $\mathrm{B}(b \to s\gamma) = (1.88 \pm 0.67) \times 10^{-4}$. Combining the two results with equal weight and taking into account the correlation in the event samples yields the result $\mathrm{B}(b \to s\gamma) = (2.32 \pm 0.51(stat.) \pm 0.29(yield) \pm 0.32(efficiency)) \times 10^{-4}$. This value is consistent with the standard model prediction; it shows no sign of enhancement from the exchange of a charged Higgs. Note, that this limit does not constrain supersymmetric models if $\tan\beta$ is large because of possible destructive interference from charginos [143]. The bounds on the Higgs mass and coupling are shown in figure 21 along with other constraints from other processes. So far there is no evidence for the existence of these particles, and the allowed parameter space is shrinking.

| Expt. | | Limit (90% C.L.) |
|---|---|---|
| CLEO | [139] | $< 2.2 \times 10^{-3}$ |
| ARGUS | [140] | $< 7.8 \times 10^{-3}$ |
| ALEPH | [137] | $< 1.5 \times 10^{-3}$ |

**Table 16.** Limits on the decay $B \to \tau\bar{\nu}$.

## 5. Conclusion

The last year has seen many elegant and detailed results that explore the standard model at ever

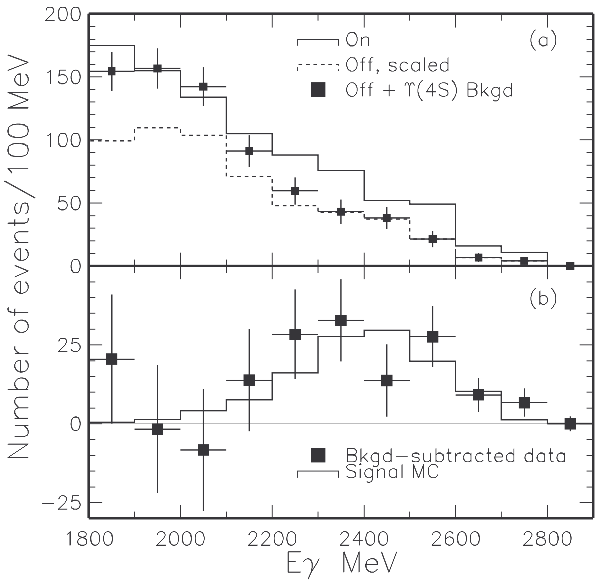


**Figure 19.** The energy spectrum of photons from the decay $b \to s\gamma$ from the analysis reconstructing the recoiling system. The upper plot shows the distributions of the data (histogram), continuum background (dashed line) and the combined $B\bar{B}$ and continuum background (filled squares); the lower plot show the background subtracted data (filled squares) with the expected signal distribution (histogram) superimposed (CLEO).

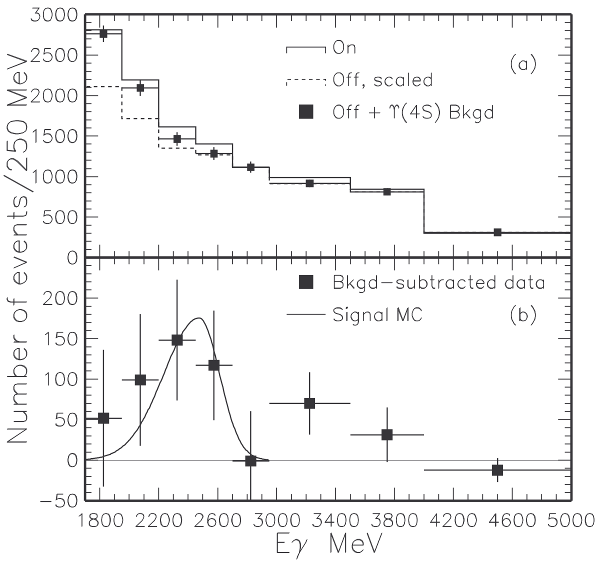


**Figure 20.** The energy spectrum of photons the decay $b \to s\gamma$ from the analysis using kinematic selection of the signal. The upper plot shows the distributions of the data (histogram), continuum background (dashed line) and the combined $B\bar{B}$ and continuum background (filled squares); the lower plot show the background subtracted data (filled squares) with the expected signal distribution (curve) superimposed (CLEO).

deeper levels. Through it all, the standard model has succeeded remarkably well in describing this microphysical world. In the coming years we will

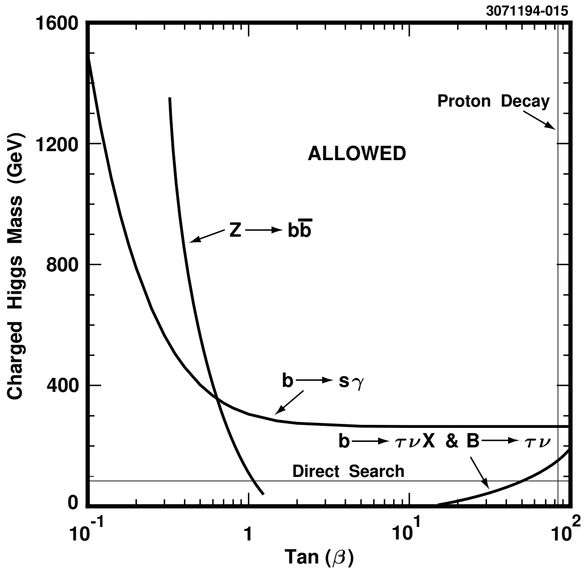


**Figure 21.** Current limits on the mass and coupling of charged Higgs' particles in two Higgs doublets models.

probe yet further, and – perhaps – glimpse physics lying beyond the standard model.

## Acknowledgments

This review benefited from the contributions of many people. I would particularly like to thank Ed Thorndike for many valuable suggestions, Jeff Richman for interesting discussions of $V_{cb}$, Lawrence Gibbons and Persis Drell for their careful reading of the manuscript and Jon Rosner and Roy Briere for interesting conversations. I would also like to thank the people who shared their experimental results, among them Jim Pilcher and Mike Roney from OPAL, Henri Videau, Vivek Sharma and Ian Scott from ALEPH, Juergen Drees and Duncan Reid from DELPHI, Robert Clare from L3, Dick Mischke from MEGA, Andrei Golutvin and Ivan Korolko from ARGUS, Joe Izen and Bill Dunwoodie from BES and John Haggerty and Stewart Smith from BNL E787.

## References


[1] R. Forty, these proceedings.
[2] P. Roudeau, these proceedings.
[3] BES Collaboration, submitted to this conference.
[4] BES Collaboration, J. Z. Bai *et al.*, Phys. Rev. Lett. **69** (1992) 3021.
[5] A. Brandelik *et al.*, Phys. Lett. **73B** (1978) 109.
[6] W. Bartel *et al.*, Phys. Lett. **77B** (1978) 331.
[7] DELCO Collaboration, W. Bacino *et al.*, Phys. Rev. Lett. **41** (1978) 13and Phys. Lett. **96B** (1980) 214.
[8] C. Blocker, Ph. D. Thesis, University of California, Berkeley, LBL-10801.

[9] ARGUS Collaboration, H. Albrecht *et al.*, Phys. Lett. **292B** (1992) 221.
[10] CLEO Collaboration, R. Balest *et al.*, Phys. Rev. **D47** (1993) R3671.
[11] OPAL Collaboration, R. Akers *et al.*, CERN preprint CERN-PPE-94-129, July, 1994; submitted to *Phys. Lett.* . This result is based on data collected during the 1990 through 1993 runs.
[12] ALEPH Collaboration, submitted to this conference. This result is based on data collected during the 1989, 1990 and 1992 runs.
[13] DELPHI Collaboration, submitted to this conference.
[14] CLEO Collaboration, C. Bebek *et al.*, Phys. Rev. **D36** (1987) 690.
[15] MAC Collaboration, H. Band *et al.*, Phys. Rev. Lett. **59** (1987) 415.
[16] ARGUS Collaboration, H. Albrecht *et al.*, Phys. Lett. **B199** (1987) 1580.
[17] HRS Collaboration, S. Abachi *et al.*, Phys. Rev. Lett. **59** (1987) 2519.
[18] TASSO Collaboration, W. Braunschweig *et al.*, Zeit. Phys. **C39** (1988) 331.
[19] MARK II Collaboration, D. Amidei *et al.*, Phys. Rev. **D37** (1988) 1750.
[20] JADE Collaboration, C. Kleinwort *et al.*, Zeit. Phys. **C42** (1989) 7.
[21] CLEO Collaboration, M. Battle *et al.*, Phys. Lett. **B291** (1992) 488.
[22] CLEO Collaboration, CLEO-CONF 94-20, submitted to this conference.
[23] SLD Collaboration, submitted to this conference.
[24] SLD Collaboration, submitted to this conference.
[25] S. Wasserbaech, Phys. Rev. **D48** (1993) 4216.
[26] J. Timmermans, these proceedings.
[27] DELPHI Collaboration, DELPHI 94-120 PHYS 437, submitted to this conference.
[28] ALEPH Collaboration, submitted to this conference.
[29] CELLO Collaboration, H. J. Behrend *et al.*, Phys. Lett. **127B** (1983) 270.
[30] PLUTO Collaboration, C. Berger *et al.*, Zeit. Phys. **C28** (1985) 1.
[31] MARK III Collaboration, R. M. Baltrusaitis *et al.*, Phys. Rev. Lett. **55** (1985) 1842.
[32] MAC Collaboration, W. W. Ash *et al.*, Phys. Rev. Lett. **55** (1985) 2118.
[33] TASSO Collaboration, M. Althoff *et al.*, Zeit. Phys. **C26** (1985) 521.
[34] JADE Collaboration, W. Bartel *et al.*, Phys. Lett. **B182** (1986) 216.
[35] MARK II Collaboration, P. Burchat *et al.*, Phys. Rev. **D35** (1987) 27.
[36] TPC Collaboration, H. Aihara *et al.*, Phys. Rev. **D35** (1987) 1553.
[37] CRYSTAL BALL Collaboration, H. Janssen *et al.*, Phys. Lett. **B228** (1989) 273.
[38] CELLO Collaboration, H. J. Behrend *et al.*, Zeit. Phys. **C46** (1990) 537.
[39] HRS Collaboration, S. Abachi *et al.*, Phys. Lett. **B226** (1989) 405.
[40] CLEO Collaboration, R. Ammar *et al.*, Phys. Rev. **D45** (1992) 3976.
[41] CLEO Collaboration, D. Akerib *et al.*, Phys. Rev. Lett. **69** (1992) 3610;Phys. Rev. Lett. **71** (1993) 3395(erratum).
[42] OPAL Collaboration, J. D. Hobbs, *Proceedings of the Second Workshop on Tau Lepton Physics*, The Ohio State University, Columbus, OH, USA, September 8-11, 1992, published by World Scientific, ed. K.K. Gan.
[43] ARGUS Collaboration, contributed to the XVI International Symposium on Lepton and Photon Interactions, Ithaca, NY, August, AIP Press, 1993, eds. P. Drell and D. Rubin.
[44] L3 Collaboration, contributed to the XVI International Symposium on Lepton and Photon Interactions, Ithaca, NY, August, AIP Press, 1993, eds. P. Drell and D. Rubin.
[45] L. Rolandi, "Precision Tests of the Electroweak Interaction," in *Proceedings of the XXVI International Conference on High Energy Physics*, August 6 -12, 1992, Dallas, TX, AIP Conference Proceedings no. 272 (1993), ed. J. R. Sanford.
[46] J. M. Roney, *Proceedings of the Second Workshop on Tau Lepton Physics*, The Ohio State University, Columbus, OH, USA, September 8-11, 1992, published by World Scientific, ed. K.K. Gan. This reference makes use of a TRIUMF measurement, D.I. Britton *et al.*, Phys. Rev. Lett. **68** (1992) 3000.
[47] Ibid; This reference makes use of the following measurements: UA1 Collaboration, Zeit. Phys. **C44** (1989) 15;UA2 Collaboration, CERN preprint CERN-PPE/91-69; and CDF Collaboration, Phys. Rev. Lett. **68** (1992) 3389.
[48] For a detailed discussion, see W. Fetscher, Phys. Rev. **D42** (1990) 1544.
[49] ARGUS Collaboration, H. Albrecht *et al.*, DESY preprint DESY-94-100, June, 1994.
[50] A. Stahl, Phys. Lett. **B324** (1994) 121.
[51] L3 Collaboration, submitted to this conference.
[52] CLEO Collaboration, S. Behrends *et al.*, Phys. Rev. **D32** (1985) 2468.
[53] MAC Collaboration, W. Ford *et al.*, Phys. Rev. **D36** (1987) 1971.
[54] ARGUS Collaboration, H. Albrecht *et al.*, Phys. Lett. **B246** (1990) 278.
[55] ALEPH Collaboration, submitted to this conference.
[56] The Particle Data Group, Phys. Rev. **D50** (1994) 1173.
[57] ARGUS Collaboration, H. Albrecht *et al.*, Phys. Lett. **B316** (1993) 608.
[58] ARGUS Collaboration, H. Albrecht *et al.*, Zeit. Phys. **C58** (1993) 61.
[59] CLEO Collaboration, J. Bartelt *et al.*, CLEO-CONF 94-21, submitted to this conference.
[60] ARGUS Collaboration, *et al.*, DESY preprint DESY-94-120, July, 1994.
[61] ALEPH Collaboration, S. W. Snow in *Proceedings of the Second Workshop on Tau Lepton Physics*, Columbus, OH, September 8 -11, 1992, ed. K.K. Gan.
[62] OPAL Collaboration, M. Sasaki, *Proceedings of the Second Workshop on Tau Lepton Physics*, The Ohio State University, Columbus, OH, USA, September 8-11, 1992, published by World Scientific, ed. K.K. Gan.
[63] L3 Collaboration, submitted to this conference.
[64] OPAL Collaboration, R. Akers *et al.*, Phys. Lett. **B328** (1994) 207.
[65] CLEO Collaboration, M. Artuso *et al.*, Phys. Rev. Lett. **72** (1994) 3762.
[66] ARGUS Collaboration, contributed to the XXIX Rencontres de Moriond, Meribel, France, March 12 - 19, 1994.
[67] CLEO Collaboration, B. Barish *et al.*, CLEO-CONF 94-22, submitted to this conference.
[68] ALEPH Collaboration, submitted to this conference.
[69] CLEO Collaboration, D. Gibaut *et al.*, Phys. Rev. Lett. **73** (1994) 934.
[70] DELPHI Collaboration, CERN preprint CERN-PPE/94-88.
[71] OPAL Collaboration, contributed to the XVI International Symposium on Lepton and Photon Interactions,

Ithaca, NY, August, AIP Press, 1993, eds. P. Drell and D. Rubin.
[72] ALEPH Collaboration, CERN preprint CERN-PPE/94-58, submitted to *Phys. Lett.* B.
[73] CLEO Collaboration, M. Battle *et al.*, Phys. Rev. Lett. **73** (1994) 1079.
[74] CLEO Collaboration, M. Athanas *et al.*, CLEO-CONF 94-23, submitted to this conference.
[75] ALEPH Collaboration, submitted to this conference.
[76] ALEPH Collaboration, CERN preprint CERN-PPE/94-59, submitted to *Phys. Lett.* B.
[77] DELPHI Collaboration, submitted to this conference.
[78] OPAL Collaboration, R. Akers *et al.*, CERN preprint CERN-PPE/94-108, to be submitted to *Phys. Lett.* B.
[79] ARGUS Collaboration, submitted to this conference.
[80] TPC/Two-Gamma Collaboration, D. A. Bauer *et al.*, Phys. Rev. **D50** (1994) 13.
[81] CLEO Collaboration, J. Gronberg *et al.*, CLEO-CONF 94-24, submitted to this conference.
[82] CLEO Collaboration, R. Balest *et al.*, CLEO-CONF 94-25, submitted to this conference.
[83] ALEPH Collaboration, submitted to this conference.
[84] DELPHI Collaboration, contributed to the XXVI International Conference on High Energy Physics, Dallas, TX, August 6 - 12,1992. See the paper by J. M. Roney in the *Proceedings.*
[85] DELPHI Collaboration, submitted to this conference.
[86] CLEO Collaboration, CLEO preprint CLEO-CONF 94-6, submitted to this conference.
[87] ARGUS Collaboration, H. Albrecht *et al.*, Phys. Lett. **B318** (1993) 397.
[88] G. Altarelli *et al.*, Nucl. Phys. **B208** (1982) 365.
[89] Crystal Ball Collaboration, K. Wachs *et al.*, Zeit. Phys. **C42** (1989) 33.
[90] Argus Collaboration, H. Albrecht *et al.*, Phys. Lett. **B249** (1990) 359.
[91] CUSB Collaboration, C. Yanagisawa *et al.*, Phys. Rev. Lett. **66** (1991) 2436.
[92] CLEO Collaboration, S. Henderson *et al.*, Phys. Rev. **D45** (1992) 2212.
[93] CLEO Collaboration, J. Bartelt *et al.*, CLEO preprint CLEO-CONF 93-19,to be published. This paper quotes $\mathbf{B(B \to x\ell\nu) = 10.65 \pm 0.05 \pm 0.33\%}$ and also $\mathbf{B(B \to c\ell\nu) = 10.48 \pm 0.07 \pm 0.33\%}$ after subtraction of the $b$ to $u$ contribution.
[94] W. Venus, "b Weak Interaction Physics in High Energy Experiments," in AIP Conference Proceedings 302, Lepton and Photon Interactions, XVI International Symposium, eds. P. Drell and D. Rubin, Ithaca, NY (1993), p.274.
[95] OPAL Collaboration, R. Akers *et al.*, CERN preprint CERN-PPE/193-106.
[96] DELPHI Collaboration, report DELPHI 94-91 PHYS 408.
[97] I. Bigi and N. G. Uraltsev, Zeit. Phys. **C62** (1994) 623.
[98] M. Shifman, N. G Uraltsev and A. Vainshtein, HEP-PH/9405207.
[99] P. Ball and U. Nierste, HEP-PH/9403407.
[100] M. Luke and M. J. Savage, Phys. Lett. **B321** (1994) 88.
[101] L3 Collaboration, submitted to this conference.
[102] M. E. Luke, Phys. Lett. **B252** (1990) 447;C. G. Boyd and D. E. Brahm, Phys. Lett. **B257** (1991) 393.
[103] M. Neubert, SLAC preprint SLAC-PUB 6362 (1993), to appear in *Phys. Rev.* .
[104] M. Neubert, CERN Report no. CERN-TH.7395/94, submitted to *Phys. Lett.* B. Neubert finds $\hat{\rho}^2 = 0.7 \pm 0.2$ using QCD sum rule results from Ref. [103] and E. Bagan, P. Ball and P. Gosdzinsky, Phys. Lett. **B301** (1993) 249.
[105] CLEO Collaboration, Cornell Lab of Nuclear Studies preprint, CLNS 94-1285, accepted for publication in *Phys. Rev.* D.
[106] ALEPH Collaboration, submitted to this conference.
[107] ARGUS Collaboration, H. Albrecht *et al.*, Zeit. Phys. **C57** (1993) 533.
[108] M. Bauer, B. Stech, M. Wirbel, Zeit. Phys. **C29** (1985) 637.
[109] N. Isgur, D. Scora, B. Grinstein, and M. B. Wise, Phys. Rev. **D39** (1989) 799.
[110] D. Atwood, B. Blok and A. Soni, SLAC preprint SLAC-PUB-6635.
[111] CLEO Collaboration, M. Athanas *et al.*, CLEO-CONF 94-2, submitted to this conference.
[112] A. Ali, V. M. Braun and H. Simma, CERN Report no. CERN-TH./7118-93.
[113] J. M. Soares, Phys. Rev. **D49** (1994) 283.
[114] S. Narison, Phys. Lett. **B327** (1994) 354.
[115] G. Buchalla and A.J. Buras, Nucl. Phys. **B412** (1994) 106.
[116] BNL E787 Collaboration, submitted to this conference.
[117] BNL E787 Collaboration, M. S. Atiya *et al.*, Phys. Rev. **D48** (1993) 1.
[118] M. Pohl, these proceedings.
[119] J. L. Ritchie, "The Status of Rare Kaon Decay Experiments," in AIP Conference Proceedings 302, Lepton and Photon Interactions, XVI International Symposium, eds. P. Drell and D. Rubin, Ithaca, NY (1993), p.1.
[120] R. Arnowitt and P. Nath, Phys. Rev. Lett. **66** (1991) 2708.
[121] MEGA Collaboration, R. D. Bolton *et al.*, Phys. Rev. **D38** (1988) 2077.
[122] CLEO Collaboration, A. Bean *et al.*, Phys. Rev. Lett. **70** (1993) 138.
[123] SINDRUM Collaboration, U. Bellgardt *et al.*, Nucl. Phys. **B299** (1988) 1.
[124] CLEO Collaboration, J. Bartelt *et al.*, Phys. Rev. Lett. **73** (1994) 1890.
[125] SINDRUM II Collaboration, submitted to this conference.
[126] B. E. Matthias *et al.*, Phys. Rev. Lett. **66** (1991) 2716.
[127] FNAL E799 Collaboration, P. Krolak *et al.*, Phys. Lett. **B320** (1994) 407.
[128] BNL E791 Collaboration, K. Arisaka *et al.*, Phys. Rev. Lett. **70** (1993) 1049.
[129] ARGUS Collaboration, H. Albrecht *et al.*, Phys. Lett. **B210** (1988) 267.
[130] CLEO Collaboration, R. Ammar *et al.*, Phys. Rev. **D49** (1994) 5701.
[131] BNL E777 Collaboration, A. M. Lee *et al.*, Phys. Rev. Lett. **64** (1990) 165.
[132] CLEO Collaboration, R. Balest *et al.*, CLEO-CONF 94-4, submitted to this conference.
[133] L3 Collaboration, O. Adriani *et al.*, Phys. Lett. **B316** (1993) 427.
[134] L3 Collaboration, submitted to this conference.
[135] P. Heiliger and L.M. Sehgal, Phys. Lett. **B229** (1989) 409.
[136] A. Falk,Z. Ligeti,M. Neubert and Y. Nir,Phys. Lett. **B326** (1994) 145.
[137] ALEPH Collaboration, PU-PHY-94/582, submitted to this conference.
[138] L3 Collaboration, M. Acciarri *et al.*, Phys. Lett. **B332** (1994) 201.
[139] CLEO Collaboration, CLEO preprint CLEO-CONF 94-5, submitted to this conference.

[140] ARGUS Collaboration,
[141] CLEO Collaboration, B. Barish *et al.*, CLEO-CONF 94-1, submitted to this conference.
[142] CLEO Collaboration, R. Ammar *et al.*, Phys. Rev. Lett. **71** (1993) 674.
[143] S. Bertolini and F. Vissani, International School for Advanced Studies, Trieste, preprint SISSA 40/94/EP, March 1994, submitted to this conference, and references therein.

## Questions

*J.H. Kühn, Karlsruhe:*
Measurements based on $\tau$ spin correlations are insensitive to the sign of the neutrino helicity, only the first measurement of ARGUS which involves a parity violating quantity is sensitive to the sign.

*J.R. Patterson:*
Thank you for this important point.

*W. Bael, Karlsruhe:*
Semileptonic branching ratios at LEP and the $\Upsilon(4S)$ are different, you are worried about systematic errors. Why should they be equal since at high energies one has a different mixture of $b$-hadrons?

*J.R. Patterson:*
Theorists tell us that the semileptonic rates of all $b$ hadrons should be similar. If I use the average $b$ hadron lifetime together with the $b$ semileptonic branching fraction, both measured at LEP, then I find a rate of $(7.3 \pm 0.04) \times 10^{10}\mathrm{sec}^{-1}$. This differs by about two standard deviations from the semileptonic rate of $(6.3 \pm 0.3) \times 10^{10}\mathrm{sec}^{-1}$ calculated from the $B$ meson semileptonic branching fraction and lifetime. Now, it is possible that the semileptonic rates of these particles are **not** the same. In particular it could be different for the $\Lambda_b$. However, since the $\Lambda_b$ accounts for only about 10% of the $b$ particles produced at LEP, its rate would have to be a factor of 1.5 larger than that of the mesons to shift the average by 5%. A rate this large is possible, but perhaps suprising.

*B.F.L. Ward, Tennessee:*
In your talk, you presented measurements of $\rho^2$, the slope of the Isgur-Wise function. Could you comment on the near term expected size of the errors on these measurements relative to the current size of the theoretical uncertainties on the predictions for $\rho^2$.

*J.R. Patterson:*
The current measurements are limited by the statistical error, so their precision should improve. Already the experimental precision is comparable to (or better than) the theoretical precision.